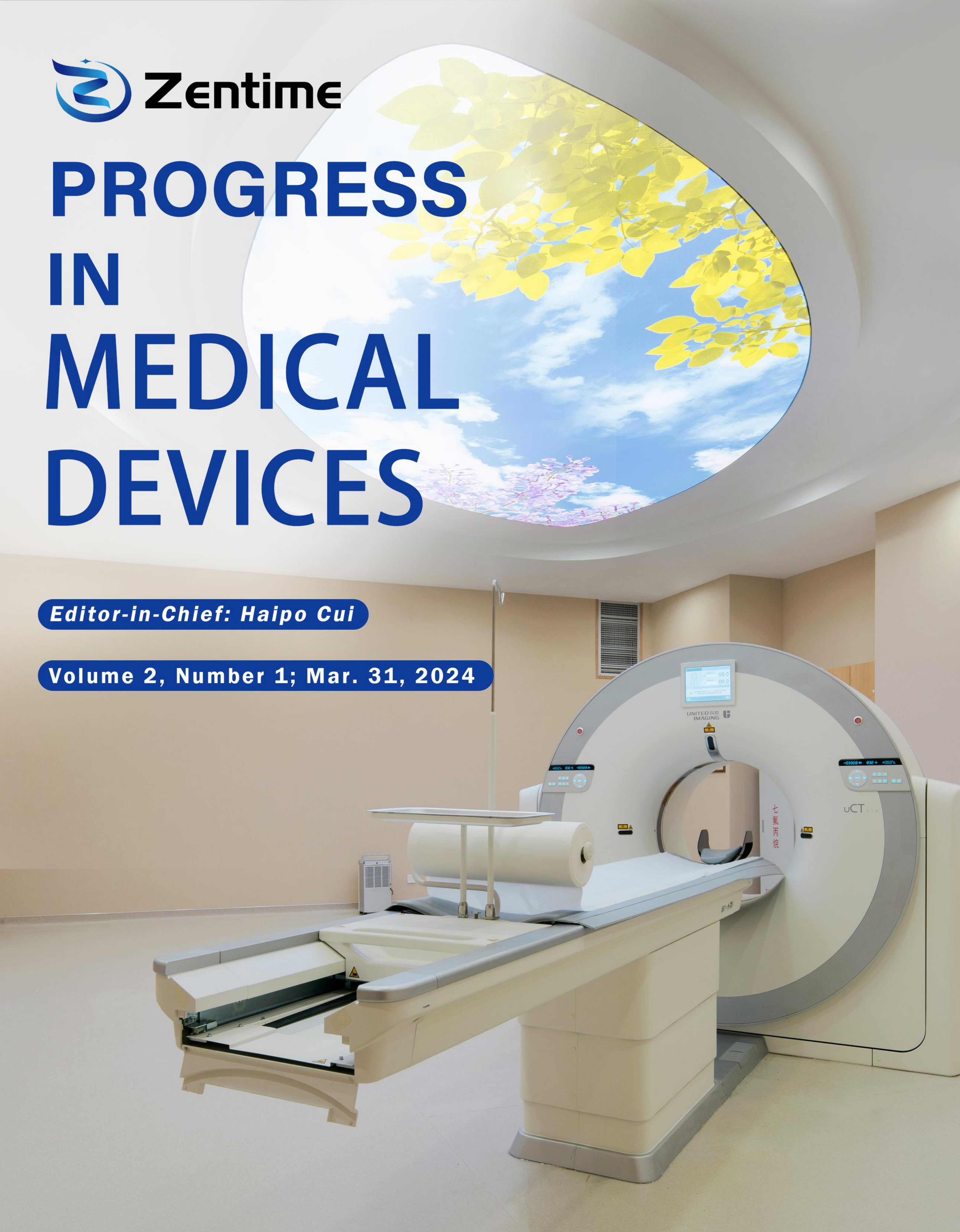

Zentime

PROGRESS IN MEDICAL DEVICES

Editor-in-Chief: Haipo Cui

Volume 2, Number 1; Mar. 31, 2024

ISSN: 2957-5478

Published by ZENTIME PUBLISHING CORPORATION

Progress in Medical Devices
eISSN: 2957-5478

Review Article https://doi.org/10.61189/295735bbiagx

The application of mammography imaging in the diagnosis and prediction of breast diseases

Siyan Liu[1,*], Guihua Wu[2,*], Changjiang Zhou[2,#], Shiju Yan[1,#], Haipo Cui[1]

[1]School of Health Sciences and Engineering, University of Shanghai for Science and Technology, Shanghai 200093, China. [2]Department of Sonography, People's Hospital Affiliated to Shandong First Medical University, Jinan 271100, Shandong, China.
[*]The authors contribute equally.

Corresponding authors: Changjiang Zhou and Shiju Yan.

Declaration of conflict of interest: None.

Received September 22, 2023; Accepted December 6, 2023; Published March 31, 2024

Highlights

Computer-assisted detection, diagnosis, and prediction systems play an effective role in diagnosing and treating female breast diseases and monitoring the course of disease. Especially in mammography imaging, they provide key support for the early diagnosis of breast cancer. This highlights the significance of modern technology in enhancing breast disease management and improving women's health.

Abstract

Breast diseases pose a significant threat to women's health, so early detection and treatment are extremely important. In this context, early disease identification has become crucial in the diagnosis and treatment of breast diseases. This paper begins by outlining the pivotal role of mammography in the early diagnosis of breast cancer, comparing the structural similarities and differences between normal and diseased breast tissues. This comparison underscores the primary role of mammography in the diagnosis and treatment of breast diseases. Additionally, our paper provides an overview of fundamental concepts related to breast cancer detection, diagnosis, and prediction systems. It delves into the latest research developments in auxiliary diagnostic detection, examination, and risk prediction systems associated with breast cancer. Our objective is to offer a comprehensive understanding of the role of computer-aided detection, diagnosis, and prediction systems in breast diseases, fostering further development and application. This work aims to explore and drive innovation in the field, enhance early detection rates of breast diseases, and guide readers towards novel directions, thus contributing to female healthcare management.

Keywords: Mammography, imaging, computer-aided diagnosis, deep learning, multi-modality

Introduction

Since 1991, the incidence of breast cancer has been on the rise, establishing it as the predominant cause of mortality among women aged 20 to 59. According to the global cancer statistics report released by the American Cancer Society in January 2023, breast cancer has become the most prevalent cancer among women. It was estimated that in 2023, there would be 300,590 new cases of breast cancer in the United States with 297,790 female cases, constituting for 31% of all cancers in women [1].

The strategies pertaining to early detection and treatment of breast cancer have garnered substantial attention and witnessed notable advancements [2]. The mortality rate linked to breast cancer in women attained its apex in 1989 and since then has exhibited a declining trajectory. This downward trend can be attributed to advancements in early detection technologies, particularly notable enhancements in mammography, ultrasound, and treatment modalities, resulting in a substantial 42% reduction in the mortality rate [3]. Practice has proven that imaging plays a very important role in the detection, diagnosis, and prediction of

[#]**Address correspondence to: Changjiang Zhou**, Department of Sonography, People's Hospital Affiliated to Shandong First Medical University, Changshao North Road, Laiwu District, Jinan 271100, China. E-mail: 390585866@qq.com/jnsrmyybgs@jn.shandong.cn. **Shiju Yan**, School of Health Science and Engineering, University of Shanghai for Science and Technology, No.516 Jungong Road, Yangpu District, Shanghai 200093, China. Tel: 18217617984. E-mail: yanshiju@usst.edu.cn.

breast diseases. Timely screening and early intervention and treatment have demonstrated significant efficacy in enhancing patient survival rates [2].

In the realm of breast disease diagnosis, the main examination methods encompass X-rays, ultrasound, MRI, computed tomography, among others. Mammography X-ray examination is simple to operate and low in cost, so it is the preferred imaging diagnostic method [4]. Computer-aided diagnosis (CAD) system, an integration of medical imaging and computer science, colloquially referred to as the "radiologist's auxiliary visual aid", is meticulously crafted to expedite the overall comprehension of mammograms by radiologists. Empirical observations have substantiated that the capacity of the CAD systems can improve the early detection rate of cancers. For example, the study by Morton and his team showed a 7.62% increase in the detection of breast cancers using CAD in cases with benign or negative results [5]. The CAD system exhibits proficiency in prognosticating the malignancy level of breast lesions. Illustratively, a study conducted by Ramadan et al. in 2016 employed a feature selection algorithm and a support vector machine classifier to analyze features such as morphology, size, and margins of breast masses to predict their malignancy, and showed an accuracy rate of 84.7% [6].

In recent times, deep learning (DL) has demonstrated significant achievements across diverse domains, encompassing applications such as automatic speech recognition and optical character recognition, natural language processing, as well as object detection, recognition, and classification. These milestones signify not only a notable progression within the sphere of machine learning but also herald a new epoch in the domain of computer vision [7]. Consequently, DL methodologies have sparked unparalleled enthusiasm in various sectors of pattern recognition and artificial intelligence (AI), notably including the domain of CAD in the field of medicine. CAD integrates machine learning techniques and interdisciplinary knowledge to analyze medical imaging and non-imaging data, facilitating the provision of analytical outcomes to clinicians. The outcomes generated by the CAD system function as a secondary evaluation or decision support for patients at diverse stages of the healthcare continuum [8]. This underscores the scalability and dependability of CAD as a decision support tool for clinicians, particularly in the realm of breast imaging applications.

This paper, firstly, introduces the detection methods of breast X-ray imaging, emphasizing its significance in the early diagnosis of breast cancer. By comparing the structures of normal and pathological breast tissues, the pivotal role of breast X-ray mammography in the diagnosis and treatment of breast diseases is elucidated. Subsequently, the article provides a brief overview of the fundamental concepts related to breast cancer detection, diagnosis, and prediction systems. It further delves into recent research developments, with a specific focus on advancements in breast cancer auxiliary diagnostic detection and risk prediction systems. The purpose of this paper is to review breast cancer CAD systems and related technologies based on mammography imaging, with an aim to attract more attention to the field of breast cancer CAD research and advance studies on breast cancer detection, diagnosis, and prediction systems.

Applicability of mammography imaging in the diagnosis and treatment of breast diseases

Imaging modalities have long been indispensable in both the initial screening and later-stage assessment of breast cancer. Currently, in the diagnostic process of breast cancer, physicians prefer non-invasive examination techniques to minimize adverse effects on patients' body. Ultrasound, mammography, and MRI are commonly employed detection modalities in the medical staff's pursuit of accurate disease determination. They can effectively participate in the process of detecting and classifying breast lesions [9]. Simultaneously, they can contribute to the preoperative staging, efficacy evaluation, and prognosis monitoring processes. Mammography images can fully reflect the anatomy of the whole breast, presenting most of the features for qualitative diagnosis, and in particular, clearly showing the micro calcified foci of breast lesions. Therefore, most studies adopt molybdenum images, a considerable number of studies utilize ultrasound images, and a minority of studies used MRI [10].

During the mammography, a patient is first palpated by an experienced doctor before film taking. The patient undergoes the routine ultrasound examination first, followed by photography. Bilateral breast axial craniocaudal (CC) view (the patient's bilateral breasts are placed flat between two splints, and the mammography X-ray is irradiated vertically from top to bottom) and the mediolateral oblique (MLO) view (the patient is placed in the upright position, placing the film beneath the breast externally, and the X-ray is projected at an angle of 45° from the lower part of the breast) are usually

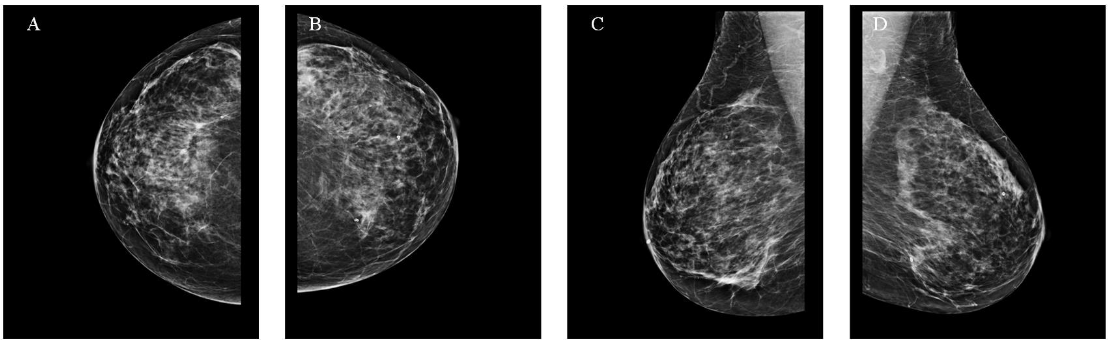

Figure 1. Example of the available views from a mammographic session. (A) Right CC view; (B) Left CC view; (C) Right MLO view; (D) Left MLO view. This figure was cited from the Chinese Mammography Database. CC, craniocaudal; MLO, medial-lateral oblique.

chosen for imaging (**Figure 1**). **Figure 1** was cited from the Chinese Mammography Database.

In mammography images depicting normal breast tissue, distinct anatomical components, such as the nipple, areola, skin, subcutaneous fat, and glandular tissue, are typically discernible. Conversely, mammographic images of patients afflicted with breast tumors often present of calcifications, masses, or a combination of both. Calcifications can manifest in both benign and malignant neoplasms. For clinicians, factors such as the size, shape, and distribution of calcifications hold diagnostic significance. Masses usually exhibit varying shape and margin distortion, presenting as round, oval, lobulated, or irregular entities with indistinct boundaries, accompanied by spiculations and infiltrations, often featuring higher densities in relation to the surrounding glandular tissue. Because breast cancer is a malignant tumor that results from the abnormal proliferation of ductal or lobular epithelial cells in breast tissue, a high prevalence is found in the breast epithelial tissue [11].

In mammography images, normal breast tissue and cancer-affected breast tissue exhibit distinct structural differences, including density, morphology, borders, and microcalcifications. Breast cancer tissue typically appears as areas of high density in mammography images, whereas normal breast tissue is characterized by uniformly distributed low-density areas [12]. Morphologically, breast cancer tissue may present as irregular nodules, patches, or masses, while normal breast tissue generally exhibits a more uniform appearance. The borders of breast cancer tissue tend to be less defined, often displaying spiculated or irregular edges, whereas the borders of normal breast tissue are clearer [13]. In mammography images, breast cancer tissue may manifest as atypical microcalcifications, a feature that is generally absent in normal breast tissue. These structural variances play a crucial role in early diagnosis and quantitative analysis of breast cancer. Early detection of breast cancer can enhance the likelihood of successful treatment and reduce the risk of patient mortality. Mammography imaging aids clinicians in detecting abnormal breast tissue and identifying potential tumors at an early stage.

With mammography imaging technology, physicians can utilize features, such as image density, morphological characteristics, boundary clarity, and microcalcifications, to identify potential abnormal tissues. With their medical expertise and clinical experience, physicians can assess these image features and make accurate diagnoses by integrating them with other clinical information. Furthermore, advanced imaging techniques, such as digital mammography and breast ultrasound, provide more detailed information about breast tissue, assisting doctors in precise diagnosis and formulating treatment plans [14].

In the diagnosis of suspected breast lesions in females, X-ray mammography and breast ultrasound exhibit comparable diagnostic accuracy, albeit with X-ray mammography images demonstrating notably higher specificity than breast ultrasound, characterized by robust targeting capabilities and heightened sensitivity. The rapid advancements in computerized imaging and digital image processing technologies have propelled the progress of mammography, yielding clearer images with enhanced contrasts [15]. Leveraging low-energy, long-wavelength X-rays with limited penetration, mammography is particularly well-suited for breast tissue examination [16]. Globally, it is widely acknowledged as the foremost screening tool for breast cancer. In the United States, mammography has been integrated into routine screenings for women as an essential diagnostic tool. Per the guidelines of the American Cancer Society, routine mammograms are recommended every one to two

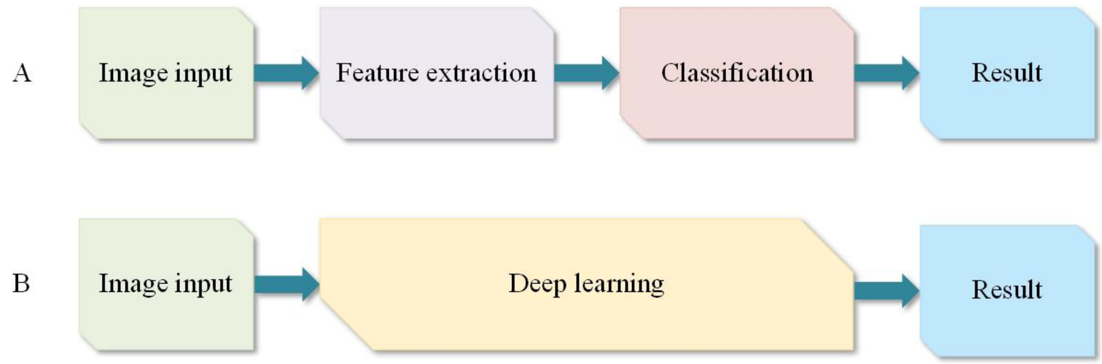

Figure 2. Traditional CAD and AI-CAD processes. (A) Human defines features: CAD; (B) AI extracts features from learning data: Deep Learning AI-CAD. CAD, computer-assisted diagnosis; AI, artificial intelligence.

years for women aged 40 to 49, which significantly enhances the early detection of breast cancer [17].

Application of mammography imaging in the diagnosis and treatment of breast diseases

Imaging technology is a crucial means for the diagnosis, staging, and assessment of breast cancer. Studies using computers to automatically analyze radiographic images emerged in the 1960s. Some researchers attempted to use computers to automatically detect breast abnormalities, a pursuit constrained by computational resource limitations and challenges associated with acquiring high-fidelity digitized image data [18]. Despite the initial feasibility of these early endeavors, they garnered limited attention. Over the subsequent five decades, significant advancements have unfolded in the domain of medical imaging technology. By 2017, a study showed that the sensitivity of breast cancer screening with mammography images had increased from 78.7% to 86.9% [19].

In the quest to enhance the lucidity of patient lesion details and enable refined and accurate diagnostic assessments, ongoing advancements in medical imaging technology persist, accompanied by a proliferation of data. Iterative reviews or the involvement of multiple radiologists in the interpretation of the same mammographic image have the potential to diminish misdiagnosis rates. However, this approach can be exceedingly labor-intensive and costly, exerting a substantial burden on healthcare systems. In 1966, Ledley proposed CAD system in an article published in Science [20]. This system integrates computer technology with medical diagnosis, utilizing robust computational capabilities to analyze medical images and assist physicians in disease diagnosis. The initial CAD systems can be categorized into two types: one is CADe that used for computer-aided detection, in which the computer annotates and indicates the location of suspected lesion areas in the medical image, followed by the doctor's diagnosis of the condition and management of the patient; and the other is CADx that used for computer-aided diagnosis, in which the preliminary task of annotating lesion areas is given to a person or a computer, with the computer generating the final diagnosis results and displaying them to the physician, such as the probability of malignancy. CAD has been used to screen mammography images for over 20 years. In recent years, the convergence of AI and computer-aided detection and diagnosis has led to the emergence of AI-CAD, which harnesses the potential of cutting-edge techniques such as machine learning and DL for intricate medical image analysis and diagnostics. By leveraging these cutting-edge technologies, AI-CAD surpasses traditional CAD systems, better comprehending the complex features of medical images and providing more accurate diagnostic results (**Figure 2**). This system not only facilitates the identification of anomalous regions but also delivers refined diagnostic recommendations based on extensive data, thereby amplifying a more significant role in clinical applications.

Overall, CADe provides comprehensive detection support, while CADx emphasizes rapid diagnosis of abnormal regions. AI-CAD, on the other hand, has made significant strides in both aspects, leveraging advanced AI technologies to enhance diagnostic accuracy and efficiency.

Mammography used in the detection of breast diseases

The purpose of CADe is to automate the localization of disease classification and to integrate the physician's judgement to form a practical and useful diagnostic prediction. Huo et al. investigated a CADe based on mammography im-

Table 1. Some neural network architectures for medical tissue segmentation and classification

Network name	Reference
CNN	Cai et al. (2020) [53] Chakravarthy and Rajaguru (2022) [54]
U-Net	Ronneberger et al. (2015) [55]
VGGNet	Simonyan and Zisserman (2014) [56]
DenseNet	Huang et al. (2017) [57]
ImageNet	Sert et al. (2017) [58]
UNETR	Hatamizadeh et al. (2022) [59]
Transunet	Chen et al. (2021) [60]
Doubleu-net	Jha et al. (2020) [61]
Swin-unet	Cao et al. (2022) [62]
Medical SAM adapter	Wu et al. (2023) [63]

Note: CNN, Convolutional Neural Network; VGG, Visual Geometry Group; UNETR, U-net Transformer.

ages, in which a radiologist or an experienced X-ray examiner manually scored the appearance of the mass in the image and then followed up with a computer [21]. In the preliminary investigation, four features, namely spiculation, edge density, and two density correlation metrics of the mass, were extracted and subsequently subjected to classification utilizing a neural network and a hybrid classifier, ultimately generating the detection outcomes. Subsequent to the initial study, Huo et al. made several iterative improvements to the methodology. The first improvement involved the application of region growing and radial edge gradients to extract spiculation features, introducing a rule-based method and the integration of an artificial neural network as a hybrid information processing approach [22]. In Huo's earlier study, they used the patient's mammography images in MLO position and head-to-tail CC position, while in the subsequent study, images in special positions (such as spot compression or spot magnification views) were also added. Studies have shown that mammography images with special views are more helpful for radiologists in distinguishing benign and malignant lesions than images with standard views [23].

Liao et al. developed a DL system based on DenseNet combined with quality algorithms [24]. The system exhibited high sensitivity in detecting breast mass, outstanding performance in diagnosing benign-malignant asymmetric lesions, and proficiency in diagnosing such lesions in both dense and non-dense breasts. This system demonstrated an excellent performance compared with junior radiologists. Balaji et al. proposed a breast cancer detection method based on Chimp Optimization Algorithm Based Type-2 Intuitionistic Fuzzy C-Means Clustering (COA-T2FCM), combining type-2 intuitionistic fuzzy C-means clustering and an oppositional function [25]. The method was tested on three datasets, exhibiting high accuracy and similarity. Similarly, Pal et al. employed a hybrid segmentation technique based on Fruitfy optimization algorithm and Fuzzy C-Means clustering, utilizing extended Gabor wavelet transform for MRI image feature extraction, enabling early diagnosis of breast cancer. Research findings indicated a superior performance and accuracy (96.50%) of the hybrid segmentation technique, holding promising implications for precise localization of breast cancer lesions [26].

The optimization of mammography imaging for breast cancer detection is fundamentally grounded in two key dimensions: patient positioning and the application of CADe strategies in image processing.

Strategically adjusting the patient's posture to an optimal position is a pivotal factor influencing the efficacy of breast X-ray mammography image detection. This adjustment is not merely a procedural formality but a critical determinant in mitigating the complexities associated with image interpretation. The optimization strategy serves not only to alleviate challenges posed by anatomical complexities but also provides a stable and reliable foundation for CADe systems.

Simultaneously, the development and application of CADe strategies offer new possibilities for optimizing diagnostic accuracy and the workflow of healthcare professionals. Beyond their conventional role as diagnostic aids, improved CADe trategies are poised to yield profound impacts, including heightened accuracy in breast cancer diagnosis, reduced cognitive burden on healthcare professionals, and alterations to existing diagnostic patterns. These advancements hold promise to simplify processes and foster an environment conducive to improving diagnostic outcomes, shaping the future landscape of breast X-ray mammography imaging in breast cancer detection. This progress not only strengthens the theoretical foundations of mammography imaging but also

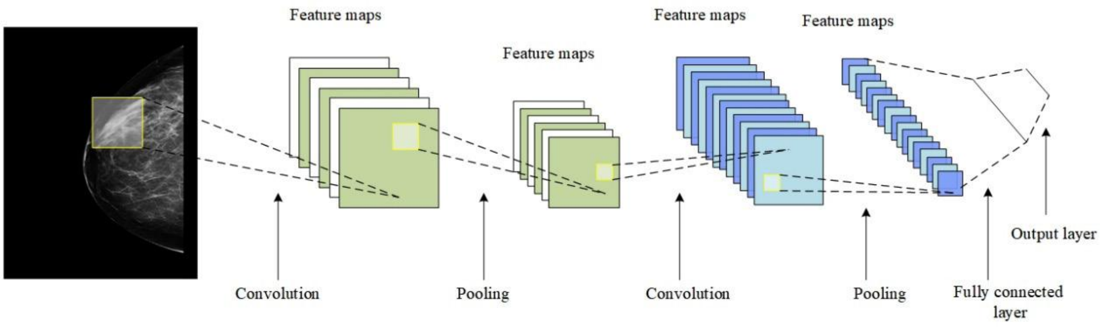

Figure 3. Convolutional neural networks. The input images in the neural network shown was cited from the Chinese Mammography Database.

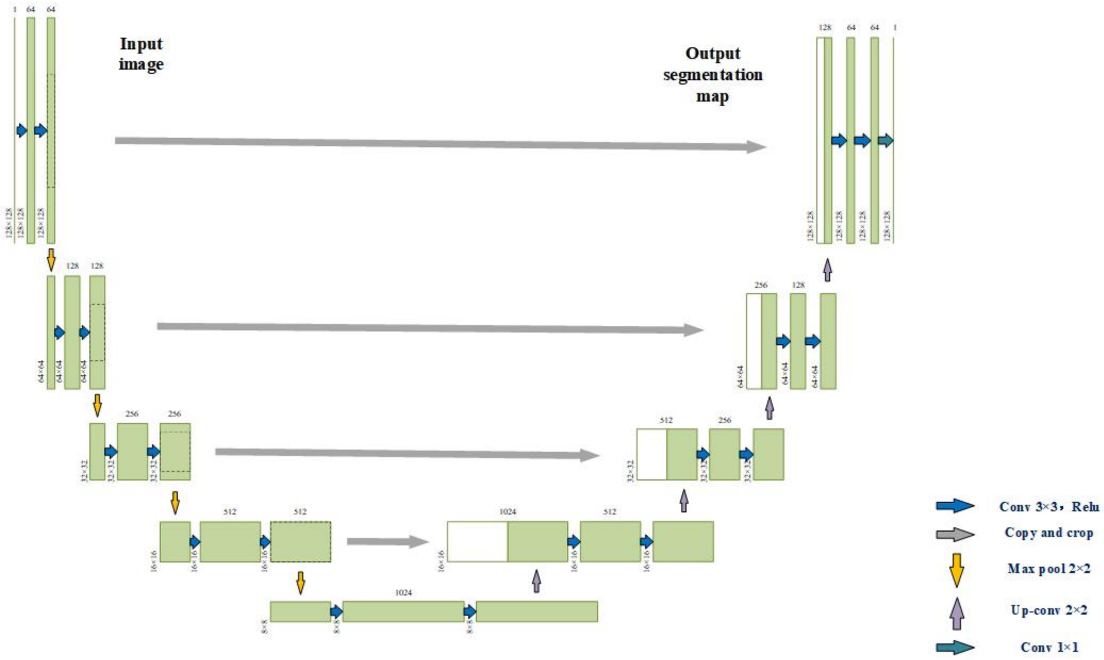

Figure 4. U-net architecture. This figure was adapted from [34].

provides valuable insights for future research and clinical practices.

Mammography used in the diagnosis of breast cancer

In the mid-1980s, the University of Chicago began to focus on CADx for the diagnosis of breast cancer based on mammography images [27]. Early-stage breast cancer usually presents tiny masses and microcalcifications that are challenging to detect in medical images. Applying CAD in the diagnosis of breast cancer can improve the accuracy of the localization and identification of lumps and calcification sites and to reduce identification errors due to the overlapping of structures or the presence of speckles in the image pictures.

Convolutional Neural Networks (CNNs), which originated as a new neural network in the early 1980s, were introduced into the field of medical image analysis in 1993 and are now widely used for solving a variety of technical problems in medical imaging (**Figure 3**) [28-30]. The input images in the neural network shown in **Figure 3** was cited from the Chinese Mammography Database. Most of studies adapted some well-known CNN architectures, such as modified versions of the architectural frameworks of AlexNet, various iterations of GoogleNet, and diverse iterations of Microsoft's ResNet, with alterations in the hyperparameters or kernel layers of the original structures [31-33]. **Table 1** lists some neural network architectures for medical tissue segmentation and classification. Drawbacks of DL include the requirement for large datasets for training and uncertainties in the diagnostic significance of many deep-learned image features. This uncertainty diminishes the interpretability of deep neural network outputs, making the assessment of the importance of imaging information and the role of each feature in classification performance rather challenging.

Almajalid et al. designed a DL framework with a segmentation architecture and applied it to the assisted diagnosis of breast cancer based on molybdenum target images called U-net (**Figure 4**) [34]. **Figure 4** is adapted from [34]. U-net is a CNN framework that has been widely adopted by numerous researchers in subsequent studies. Given the significant time cost associated with manual segmentation, automatic segmentation of images has become an inevitable trend. Ragab et al. devised an ensemble deep-learning-enabled clinical decision support system for breast cancer diagnosis and classification (EDLCDS-BCDC) on ultrasound images, which incorporates chaotic krill herd algorithm and Kapur entropy techniques and uses optimal multilevel thresholding for image segmentation to identify regions affected by tumors [9]. Integration of three DL models (Visual Geometry Group (VGG)-16, VGG-19, and SqueezeNet) is used for feature extraction. Cat swarm optimization based on the multi-layer perceptron model is also used to classify breast cancer images to determine the presence of cancer. In contrast to the current prevalent learning approach, Chaudhury introduced a novel DL framework for diagnosing and classifying breast cancer using the concept of transfer learning [35]. Migration learning aims to acquire specific information from one problem to solve other similar problems. As a result, Chaudhury designed an attribute mining structure that uses CNN architectures such as GoogleNet, VGGNet, and residual networks that have been previously trained and fed into a fully linked layer to classify malignant and benign cells using an average pooling classification method. Wang et al. proposed a new model named DisAsymNet, employing self-adversarial learning guided by an asymmetric attention transformer to understand the differences between asymmetric and symmetric images for classification and diagnosis [36].

Qi et al. developed an automatic breast cancer diagnosis system that can be installed on a smartphone [37]. The scheme used molybdenum target images as input. Firstly, noise in the captured images was reduced, and high-quality images were reconstructed. Then, an initial subsystem was designed using a stacked denoising autoencoder framework and a generative adversarial network. Ultimately, a deep convolutional neural network was employed to capture the high-level features of the images and conduct binary classification of breast images, discerning between benign and malignant diagnoses. Ting et al. recommended a convolutional neural network algorithm to improve the classification of breast cancer laceration, which helps professionals diagnose the disease and classify the molybdenum images as benign, malignant, or healthy [38]. Kaur et al. developed a new algorithm with multiple support vector machines (MSVM) and DL mechanisms as the basis for proposing an automated system for breast cancer molybdenum images using k-mean clustering, and MSVM hybrid accelerated the recovery of features to obtain better classification results [39]. Following rigorous quantitative analysis and experimental validation, the study recommended the adoption of a multi-layer perceptron and J48+K mean clustering WEKA approach to achieve heightened accuracy. Baccouche et al. investigated an end-to-end based You Only Look Once (YOLO) fusion model for breast lesion detection and classification [40]. Their results indicated that using the YOLO model held promise in capturing overlooked lesions in early screening views that were clearly visible in the latest screening images.

Within the domain of CADx for diagnosing breast cancer through mammography images, it becomes apparent that the predominant strategies center on the DL-based classification of benign and malignant cancer images, as well as the segmentation of lesions within these images. Simultaneously, apart from efforts aimed at augmenting the precision of neural network diagnostic outcomes, there is a discernible research emphasis on the lightweighting network models [41].

This highlights a theoretical framework wherein the primary emphasis lies in the application of DL methodologies for the classification of breast cancer images and the delineation of lesions, underscoring a pivotal role for AI in diagnostic processes [42]. Concurrently, the research thrust towards lightweighting network models reflects a strategic exploration into optimizing computational efficiency without compromising diagnostic accuracy. This dual focus on classification and lightweighting is indicative of a nuanced approach within theoretical frameworks, aiming to balance diagnostic efficacy with computational feasibility in the context of breast cancer diagnosis through CADx methodologies.

Mammography used in the prediction of breast cancer

In recent years, research efforts have not only been dedicated to the advancement of medical imaging technology and the enhancement of image clarity but have also embraced the integration of multimodal information. This includes the integration of textual and image data into the research scope, aiming to establish breast cancer risk prediction models. These models enable risk assessment and screening for high-risk individuals, facilitating targeted intervention measures.

For instance, Kyono et al. developed a machine learning approach to identify normal cases in screening mammography [43]. Utilizing a Deep Convolutional Neural Network with multitask learning, it was trained to extract imaging features for prediction. The predictions from multiple views were combined with non-imaging patient data and input into another deep network for assessing case abnormalities. Kumar used the voting classifier technique to predict breast cancer and proposed a new model combining three classifiers, J48, Bayesian, and support vector machine, and used the voting fusion technique in the classification of benign and malignant tumors [44]. The study by Akselrod-Ballin et al. combined machine learning and DL to apply mammography images and electronic health records to construct a risk prediction model based on imaging histological features and clinical histological features [45]. The research employed standard breast image views alongside comprehensive clinical history as input, extracting medical imaging features and clinical case attributes as feature sets. By combining the eXtreme Gradient Boosting method and the minimum area under the Receiver Operating Characteristic curve method, the predictive results were binarily classified as cancer-positive or normal. Their model outperformed the commonly used Gail model, exhibiting superior sensitivity and specificity compared to the established benchmarks of the breast cancer surveillance consortium.

A team of researchers from the Computer Science and Artificial Intelligence Laboratory at the University of Massachusetts Institute of Technology and Massachusetts General Hospital has created a DL model capable of automatically predicting whether a patient is likely to develop breast cancer within the next five years based on mammographic images [46]. The utilized model incorporated full-field-of-view mammography images and considered several conventional risk factors, encompassing breast cancer diagnosis, imaging follow-up spanning at least five years post-diagnosis, age, weight, height, age at menarche, menopausal status, comprehensive family history of breast and ovarian cancer, BRCA mutation status, history of atypical hyperplasia, history of lobular carcinoma in situ, and breast density. The results demonstrated that the model was able to learn subtle patterns of malignancy signs in breast tissue with a 13% improvement in accuracy over the current clinical standard, the Tyrer-Cusick model (version 8). The study has also re-affirmed that mammograms and traditional risk factors contain complementary information and that traditional risk factors can also have a critical impact on breast cancer developement.

Qian et al. proposed a multi-path DL architecture based on multi-modal breast ultrasound images [47]. Their dataset selected patients with three imaging modes: ultrasound B-mode, color Doppler ultrasound, and elastography. Different weights were assigned to images from different imaging modes in the predictive model. Their research showed that the AI model was as good at predicting breast cancer risk as the 7 experienced radiologists in the study. Ali et al. introduced a label-free breast cancer detection tool based on a small data set [48]. The image data set used a combination of three nonlinear imaging modes (coherent anti-Stokes Raman-scattering, two-photon excited autofluorescence, and second harmonic generation), demonstrating that multi-modal imaging can improve the efficiency and accuracy of predictive diagnosis for small sample sizes of patients. Siviengphanom et al. demonstrated that the overall radiological profile of mammograms could be used to predict difficult-to-interpret cases and that a model that used either CC-view or MLO-view images alone was more accurate than a model used both CC and MLO views [49]. It was suggested that model with dual CC+MLO bits had lower performance, and quantitative overall radiomic features extracted from mammograms could help to accurately differentiate between hard-to-interpret normal cases and easy-to-interpret normal cases.

The assessment of bilateral breast asymmetry holds significance in the evaluation of cancer risk, as the presence of tumors often induces asymmetry in breast size. Studies by Li et al. have successively proposed breast cancer short-term risk prediction models based on local regional bilateral asymmetry features, and on global regional features combined with local regional features [50, 51]. Furthermore, the research conducted by Wengert et al. substantiates the pivotal role of a comprehensive evaluation of multimodal imaging in enhancing the accuracy of breast density measurement [52]. Breast density, as identified through multimodal imaging, emerges as a promising factor for risk prediction and stratification in the context of breast cancer.

In the realm of breast disease prediction, the application of mammography images has become a focal and highly discussed topic. By integrating mammography images with multimodal imaging, such as ultrasound images, and incorporating patient pathological information, we are advancing toward achieving a more precise prediction of breast diseases.

This discourse emphasizes the pivotal role of utilizing mammography images in breast disease prediction. The effective integration of these images with other modalities or patient pathology data provides us with a deliberate strategy to enhance the accuracy of auxiliary predictions. It underscores the potential synergies between different sources of medical information in shaping the theoretical framework for advancing breast disease prediction.

Conclusion and outlook

CAD plays a crucial role in the research and development of medical imaging, particularly in the field of mammography with molybdenum target images. Firstly, through a comprehensive examination of patient positioning, we can better understand how to improve the readability of molybdenum target images and the accuracy of breast disease diagnosis. Appropriate imaging positions can effectively enhance the display of breast morphology and details, assisting doctors in more accurately identifying and diagnosing breast diseases. Simultaneously, through the study of lightweight network models, it is possible to optimize the computational efficiency of models without compromising diagnostic accuracy, making it more practical for real-world applications and providing better support for molybdenum-targeted breast disease auxiliary diagnosis systems. By improving the performance of neural networks, we will further enhance the accuracy of breast disease diagnosis based on molybdenum target images, potentially predicting the likelihood of breast diseases. Finally, in the field of breast disease prediction, the integration of mammography images with other modal imaging and patient pathological information can further improve the prediction accuracy. However, despite some progress, continued in-depth research is needed to further optimize the performance of CAD systems and enhance their practical value in clinical practice.

References

[1] Siegel RL, Miller KD, Wagle NS, et al. Cancer statistics, 2023. CA Cancer J Clin 2023;73:17-48.

[2] Wilson J, Sule AA. Disparity in early detection of breast cancer. Treasure Island (FL). StatPearls Publishing, 2020.

[3] Siegel RL, Miller KD, Fuchs HE, et al. Cancer statistics, 2022. CA Cancer J Clin 2022;72:7-33.

[4] Ammar MB, Ayachi FL, de Paiva AC, et al. Harnessing Deep Learning for Early Breast Cancer Diagnosis: A Review of Datasets, Methods, Challenges, and Future Directions. Int J Comput Digital Syst 2024;15:1-13.

[5] Morton MJ, Whaley DH, Brandt KR, et al. Screening mammograms: interpretation with computer-aided detection-prospective evaluation. Radiology 2006;239:375-383.

[6] Ramadan SZ. Methods Used in Computer-Aided Diagnosis for Breast Cancer Detection Using Mammograms: A Review. J Healthc Eng 2020;2020:9162464.

[7] Esteva A, Chou K, Yeung S, et al. Deep learning-enabled medical computer vision. NPJ Digit Med 2021;4:5.

[8] Chan HP, Samala RK, Hadjiiski LM, et al. Deep learning in medical image analysis. Adv Exp Med Biol 2020;3-21.

[9] Ragab M, Albukhari A, Alyami J, et al. Ensemble Deep-Learning-Enabled Clinical Decision Support System for Breast Cancer Diagnosis and Classification on Ultrasound Images. Biology (Basel) 2022;11:439.

[10] Zhang X, Guo H. Research on an improved algorithm for image dehazing in underground coal mine. Journal of Physics: Conference Series (1693): The 2020 3rd International Conference on Computer Information Science and Artificial Intelligence (CISAI) 2020 25-27 September 2020, Inner Mongolia, China. IOP Publishing 2020;012153.

[11] Harbeck N,Gnant M. Breast cancer. Lancet 2017;389:1134-1150.

[12] Shrivastava N, Bharti J. Breast tumor detection and classification based on density. Multimed Tools Appl 2020;79:26467-26487.

[13] Durur Subaşı I. Breast imaging for non-radiologists. Erciyes Med J 2022;44:129-137.

[14] Arıbal E. Future of Breast Radiology. Eur J Breast Health 2023;19:262.

[15] Nyayapathi N. Development of Photoacoustic Technologies for Breast Cancer Imaging. New York (US). State University of New York 2020.

[16] Zhong LC, Yang T, Gu LP, et al. The diagnostic performance of shear wave velocity ratio for the differential diagnosis of benign and malignant breast lesions: Compared with VTQ, and mammography. Clin Hemorheol Microcirc 2021;77:123-131.

[17] Monticciolo DL. Current guidelines and gaps

in breast cancer screening. J Am Coll Radiol 2020;17:1269-1275.
[18] Winsberg F, Elkin M, Macy Jr J, et al. Detection of radiographic abnormalities in mammograms by means of optical scanning and computer analysis. Radiology 1967;89:211-215.
[19] Lehman CD, Arao RF, Sprague BL, et al. National performance benchmarks for modern screening digital mammography: update from the Breast Cancer Surveillance Consortium. Radiology 2017;283:49.
[20] Ledley RS. High-speed automatic analysis of biomedical pictures. Science 1964;146:216-223.
[21] Huo Z, Giger ML, Vyborny CJ, et al. Automated computerized classification of malignant and benign masses on digitized mammograms. Acad Radiol 1998;5:155-168.
[22] Huo Z, Giger ML, Vyborny CJ, et al. Analysis of spiculation in the computerized classification of mammographic masses. Med Phys 1995; 22:1569-1579.
[23] Huo Z, Giger ML,Vyborny CJ. Computerized analysis of multiple-mammographic views: Potential usefulness of special view mammograms in computer-aided diagnosis. IEEE Trans Med Imaging 2001;20:1285-1292.
[24] Liao T, Li L, Ouyang R, et al. Classification of asymmetry in mammography via the DenseNet convolutional neural network. Eur J Radiol Open 2023;11:100502.
[25] Balaji P, Muniasamy V, Bilfaqih SM, et al. Chimp Optimization Algorithm Influenced Type-2 Intuitionistic Fuzzy C-Means Clustering-Based Breast Cancer Detection System. Cancers 2023;15:1131.
[26] Pal S, Maity S, Adhikari S, et al. Breast Cancer Detection Using Hybrid Segmentation Using FOA and FCM Clustering. Proceedings of Springer (1450): Proceedings of 3rd International Conference on Mathematical Modeling and Computational Science. ICMMCS 2023. Advances in Intelligent Systems and Computing. Springer Cham 2023;65-78.
[27] Giger ML, Doi K, MacMahon H. Image feature analysis and computer□aided diagnosis in digital radiography. 3. Automated detection of nodules in peripheral lung fields. Med Phys 1988;15:158-166.
[28] Fukushima K, Miyake S. Neocognitron: A new algorithm for pattern recognition tolerant of deformations and shifts in position. Pattern Recognit 1982;15:455-469.
[29] Lo SCB, Lin JS, Freedman MT, et al. Computer-assisted diagnosis of lung nodule detection using artificial convoultion neural network. Proceedings of SPIE (1898): Medical Imaging 1993: Image Processing 1993;859-869.
[30] Zhang W, Li R,Deng H, et al. Deep convolutional neural networks for multi-modality isointense infant brain image segmentation. Neuroimage 2015;108:214-224.
[31] Fujita H. AI-based computer-aided diagnosis (AI-CAD): the latest review to read first. Radiol Phys Technol 2020;13:6-19.
[32] Szegedy C, Liu W, Jia Y, et al. Going deeper with convolutions. 2015 IEEE Conference on Computer Vision and Pattern Recognition (CVPR) 2015;1-9.
[33] He K, Zhang X, Ren S, et al. Deep residual learning for image recognition. Proceedings of the IEEE conference on computer vision and pattern recognition 2016;770-778.
[34] Almajalid R, Shan J, Du Y, et al. Development of a deep-learning-based method for breast ultrasound image segmentation. 2018 17th IEEE International Conference on Machine Learning and Applications (ICMLA) 2018; 1103-1108.
[35] Chaudhury S, Shelke N, Sau K, et al. A Novel Approach to Classifying Breast Cancer Histopathology Biopsy Images Using Bilateral Knowledge Distillation and Label Smoothing Regularization. Comput Math Methods Med 2021;2021:4019358.
[36] Wang X, Tan T, Gao Y, et al. DisAsymNet: Disentanglement of Asymmetrical Abnormality on Bilateral Mammograms Using Self-adversarial Learning. Proceedings of Springer (14226): Medical Image Computing and Computer Assisted Intervention – MICCAI 2023. Cham. Springer Cham 2023;57-67.
[37] Qi X, Yi F, Zhang L, et al. Computer-aided diagnosis of breast cancer in ultrasonography images by deep learning. Neurocomputing 2022;472:152-165.
[38] Ting FF, Tan YJ, Sim KS. Convolutional neural network improvement for breast cancer classification. Expert Syst Appl 2019;120:103-115.
[39] Kaur P, Singh G, Kaur P. Intellectual detection and validation of automated mammogram breast cancer images by multi-class SVM using deep learning classification. Inform Med Unlocked 2019;16:100151.
[40] Baccouche A, Garcia-Zapirain B, Zheng Y, et al. Early detection and classification of abnormality in prior mammograms using image-to-image translation and YOLO techniques. Comput Methods Programs Biomed 2022;221:106884.
[41] Mall PK, Singh PK, Srivastav S, et al. A comprehensive review of deep neural networks for medical image processing: Recent developments and future opportunities. Healthc Anal 2023;100216.
[42] Ranjbarzadeh R, Dorosti S, Ghoushchi SJ, et

al. Breast tumor localization and segmentation using machine learning techniques: Overview of datasets, findings, and methods. Comput Biol Med 2023;152:106443.
[43] Kyono T, Gilbert FJ,van der Schaar M. Improving workflow efficiency for mammography using machine learning. J Am Coll Radiol 2020;17:56-63.
[44] Kumar UK, Nikhil MS,Sumangali K. Prediction of breast cancer using voting classifier technique. 2017 IEEE international conference on smart technologies and management for computing, communication, controls, energy and materials (ICSTM) 2017;108-114.
[45] Akselrod-Ballin A, Chorev M, Shoshan Y, et al. Predicting Breast Cancer by Applying Deep Learning to Linked Health Records and Mammograms. Radiology 2019;292:331-342.
[46] Yala A, Lehman C, Schuster T, et al. A deep learning mammography-based model for improved breast cancer risk prediction. Radiology 2019;292:60-66.
[47] Qian X, Pei J, Zheng H, et al. Prospective assessment of breast cancer risk from multimodal multiview ultrasound images via clinically applicable deep learning. Nat Biomed Eng 2021;5:522-532.
[48] Ali N, Quansah E, Köhler K, et al. Automatic label-free detection of breast cancer using nonlinear multimodal imaging and the convolutional neural network ResNet50. Transl Biophotonics 2019;1:e201900003.
[49] Siviengphanom S, Gandomkar Z, Lewis SJ, et al. Global Radiomic Features from Mammography for Predicting Difficult-To-Interpret Normal Cases. J Digit Imaging 2023;36:1541-1552.
[50] Li Y, Fan M, Cheng H, et al. Assessment of global and local region-based bilateral mammographic feature asymmetry to predict short-term breast cancer risk. Phys Med Biol 2018;63:025004.
[51] Li Y, Fan M, Liu S, et al. Prediction of Short-Term Breast Cancer Risk Based on Deep Convolutional Neural Networks in Mammography. J Med Imaging Health Inform 2019;9:1663-1672.
[52] Wengert GJ, Helbich TH, Leithner D, et al. Multimodality Imaging of Breast Parenchymal Density and Correlation with Risk Assessment. Curr Breast Cancer Rep 2019;11:23-33.
[53] Cai G, Guo Y, Chen W, et al. Computer-aided detection and diagnosis of microcalcification clusters on full field digital mammograms based on deep learning method using neutrosophic boosting. Multimed Tools Appl 2020;79:17147-17167.
[54] Chakravarthy SS, Rajaguru H. Automatic detection and classification of mammograms using improved extreme learning machine with deep learning. Innov Res BioMed Eng 2022;43:49-61.
[55] Ronneberger O, Fischer P, Brox T. U-net: Convolutional networks for biomedical image segmentation. Proceedings of Springer (9351): Medical Image Computing and Computer-Assisted Intervention – MICCAI 2015. Springer Cham 2015;234-241.
[56] Simonyan K, Zisserman A. Very deep convolutional networks for large-scale image recognition (Preprint). ArXiv 2015.
[57] Huang G, Liu Z, Van Der Maaten L, et al. Densely connected convolutional networks. 2017 IEEE Conference on Computer Vision and Pattern Recognition (CVPR) 2017;4700-4708.
[58] Sert E, Ertekin S, Halici U. Ensemble of convolutional neural networks for classification of breast microcalcification from mammograms. 2017 39th Annual International Conference of the IEEE Engineering in Medicine and Biology Society (EMBC) 2017;689-692.
[59] Hatamizadeh A, Tang Y, Nath V, et al. UNETR: Transformers for 3d medical image segmentation. 2022 IEEE/CVF Winter Conference on Applications of Computer Vision (WACV) 2022;574-584.
[60] Chen J, Lu Y, Yu Q, et al. Transunet: Transformers make strong encoders for medical image segmentation (Preprint). ArXiv 2021.
[61] Jha D, Riegler MA, Johansen D, et al. Doubleu-net: A deep convolutional neural network for medical image segmentation. 2020 IEEE 33rd International symposium on computer-based medical systems (CBMS) 2020;558-564.
[62] Cao H, Wang Y, Chen J, et al. Swin-Unet: Unet-Like Pure Transformer for Medical Image Segmentation. Proceedings of Springer (13803): Computer Vision–ECCV 2022 Workshops. Springer Cham 2023;205-218.
[63] Wu J, Fu R, Fang H, et al. Medical sam adapter: Adapting segment anything model for medical image segmentation (Preprint). ArXiv 2023.

Progress in Medical Devices
eISSN: 2957-5478

Review Article https://doi.org/10.61189/581835yrfifv

Application of vibration analysis for medical diagnosis

Walid Mohamedi

National School of Applied Sciences, Cady Ayaed University, Morroco

Corresponding author: Walid Mohamedi

Declaration of conflict of interest: None.

Received November 15, 2023; Accepted January 30, 2024; Published March 31, 2024

Highlights

- The application of vibration analysis in medical diagnosis offers a diverse range of benefits, from non-invasive diagnostics to early detection and continuous monitoring of various health conditions.
- As technology continues to advance, the integration of vibration analysis into medical practices holds promise for enhancing diagnostic accuracy and improving patient outcomes.

Abstract

The ability to interpret vibration signals in the biomedical field offers a promising path toward continuous improvement of medical devices. By examining the revolutions per minute profile, analysts can identify any deviations or anomalies in the vibration patterns at different speeds. This information can help identify potential faults or imbalances within the rotating machinery. With a comprehensive understanding of the revolutions per minute profile, analysts can make informed decisions regarding maintenance and repairs. Besides, the analysis of the order of vibration signals represents an essential pillar of biomedical engineering, bringing an innovative and in-depth perspective to the development of medical devices, and contributing to the continued advancement of medical technology and healthcare. Integrating vibration analysis into preventive maintenance practices can help ensure the reliability of medical equipment, reduce potential risks to patients, and contribute to the advancement of healthcare quality.

Keywords: Vibration analysis, medical devices, biomedical

Introduction

Vibration is a common phenomenon in various mechanical systems and structures, ranging from rotating machinery like motors, pumps, and turbines to bridges, buildings, and vehicles [1-3]. When a mechanical system operates, it generates vibrations because of imbalances, misalignments, wear, resonance, structural weaknesses, or other mechanical faults [4-7].

Vibration analysis is a vital technique used to assess the condition and performance of machinery and structures [8-12]. It involves measurement, analysis, and interpretation of vibration signals to identify potential problems, such as faults, anomalies, or mechanical problems [13-19]. Vibration analysis utilizes specialized sensors, such as accelerometers, to capture the vibrations induced by systems or structures [20-22]. These sensors measure the acceleration, velocity, or displacement of the vibrating component and convert the mechanical vibrations into electrical signals [23-25]. Once the vibration signals are obtained, they are analyzed using various techniques and tools, including time-domain analysis, frequency-domain analysis, statistical analysis, wavelet analysis, and advanced signal processing algorithms [26-28]. The goal of vibration analysis is to extract meaningful information from the vibration signals to understand the behavior, diagnose any faults or anomalies, and make informed decisions regarding maintenance and repair [29-31].

The key objectives of vibration analysis include:

- **Fault detection:** Identifying faults or anomalies in machinery or structures. This involves detecting issues like unbalance, misalignment, bearing wear, gear damage, resonance, and mechanical looseness.

Address correspondence to: Walid Mohamedi, National School of Applied Sciences, Cady Ayaed University, Morroco, Av Abdelkrim Khattabi, B.P. 511 – 40000, Marrakech 4000, Morocco, E-mail: faouz111111@yahoo.fr.

• **Fault diagnosis:** Determining the specific nature, location, and severity of faults. By analyzing the vibrational characteristics, frequency components, and patterns, fault diagnosis aims to pinpoint the source and identify the underlying causes of the problems identified.

• **Condition monitoring:** Regularly monitoring the vibration signals to track changes in machinery performance over time. Condition monitoring enables the identification of gradual deterioration, allowing for predictive maintenance and preventing unexpected failures or breakdowns.

• **Performance optimization:** Assessing the performance of machinery or structures to maximize efficiency, minimize energy consumption, improve productivity, and extend equipment lifespan. Vibration analysis can reveal opportunities for optimization and suggest improvements to enhance performance.

• **Structural health monitoring:** Evaluating the condition and performance of structures, such as bridges, buildings, and wind turbines, to ensure their integrity and safety. Vibration analysis can detect signs of degradation, fatigue, or damage, enabling proactive maintenance and preventing catastrophic failures.

Order analysis stands as a crucial technique in the realm of vibration analysis, particularly in examining the vibrational signals emitted by rotating machinery. This methodology centers around the analysis of the signals in terms of rotational orders, which are harmonics corresponding to the fundamental rotational frequency of a rotating component, be it a gear or a shaft [32-35].

In essence, rotational orders encapsulate the multiples of the basic rotational frequency, unveiling a comprehensive perspective on the dynamic behavior of the machinery. By employing order analysis, engineers and maintenance professionals can gain valuable insights into the condition of the rotating components. This technique is proven to be indispensable for identifying specific fault frequencies, aiding in the accurate diagnosis of potential issues, and facilitating ongoing monitoring efforts [36].

In practical terms, order analysis involves processing vibration data to discern the presence and amplitude of rotational orders [37]. This information is instrumental in pinpointing irregularities, such as misalignments, unbalances, or bearing defects, that may affect the rotating machinery. The ability to isolate and interpret these harmonics provides a powerful diagnostic tool, contributing to proactive maintenance practices and the optimization of machinery reliability [38-40].

Ultimately, order analysis emerges as a vital component of predictive maintenance strategies, offering a nuanced understanding of the vibrational characteristics inherent in rotating machinery. Its applications extend across various industries, playing a pivotal role in ensuring operational efficiency, reducing downtime, and enhancing the overall reliability of critical rotating components [41-43].

Medical diagnosis by vibration analysis

Vibration analysis can be a valuable tool in medical diagnosis, providing insights into the mechanical properties of tissues and aiding in the detection and characterization of various medical conditions. Here are some specific applications of vibration analysis in medical diagnosis:

• **Elastography:** Elastography techniques use controlled vibrations to evaluate the stiffness of tissues. The presence of abnormal stiffness may indicate diseases such as liver fibrosis, breast tumors, and prostate cancer.

• **Ultrasound vibro-acoustography:** Combining ultrasound and vibration analysis, vibro-acoustography can provide detailed images of tissue structures and aid in the diagnosis of breast lesions, thyroid nodules, and other abnormalities.

• **Vibration analysis in orthopedics:** Assessing joint function and bone health by analyzing vibrations during movement can help diagnose conditions such as osteoarthritis and osteoporosis.

• **Vocal cord vibrations:** Analyzing vibrations in the vocal cords can help diagnose voice disorders and assess laryngeal health. This is particularly important in otolaryngology.

• **Cardiovascular vibration analysis:** Assessing the vibrations associated with blood flow dynamics aids in understanding cardiovascular conditions, such as detecting abnormal heart valve function and studying arterial stiffness.

• **Eye biomechanics:** Vibration analysis can be applied to study the biomechanics of the eye, aiding in the diagnosis of glaucoma and evaluating corneal health.

• **Dental diagnostics:** Analyzing vibrations in

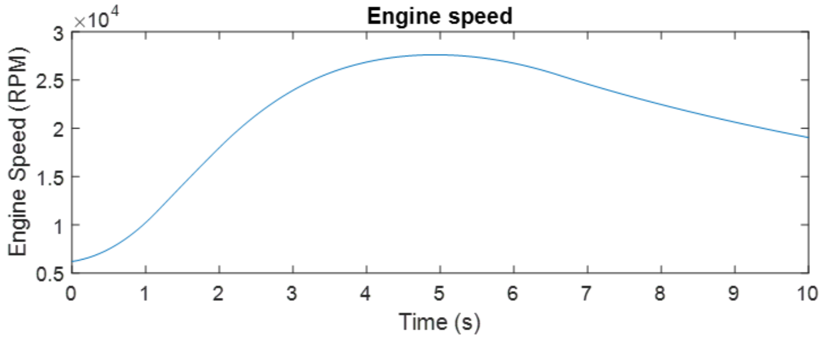

Figure 1. Motor speed as a function of time.

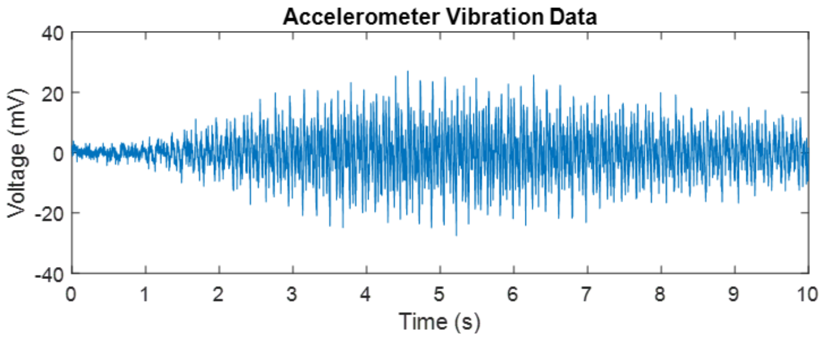

Figure 2. Accelerometer vibration data as a function of time.

teeth and jaws can assist in diagnosing dental conditions, including tooth fractures, bite forces, and temporomandibular joint disorders.

• **Vibration-based diagnostics in neurology:** Vibration analysis can be used to assess peripheral nerve function, helping diagnose carpal tunnel syndrome, diabetic neuropathy, etc.

• **Respiratory system analysis:** Analyzing vibrations associated with breathing patterns can aid in diagnosing respiratory diseases, such as asthma or chronic obstructive pulmonary disease.

• **Detection of abnormalities in organs:** Vibration analysis, when combined with imaging modalities, can help detect abnormalities in organs, such as tumors or cysts, by studying their mechanical properties.

• **Gastrointestinal system assessment:** Vibration analysis can be applied to assess the motility of the gastrointestinal tract, aiding in the diagnosis of irritable bowel syndrome and gastroparesis. etc.

In each of these applications, vibration analysis provides additional diagnostic information that complements traditional imaging techniques, contributing to more accurate and comprehensive medical assessments. The continuous exploration in vibration analysis can contribute to the improvement of diagnostic capabilities in various medical specialties.

Order analysis of a vibration signal in the field of biomedical engineering

Analysis of the order of a vibration signal is of crucial importance in the field of biomedical engineering, especially in the medical devices assisted diagnosis. This approach allows a detailed assessment of the vibration signals emitted by medical devices, providing valuable information on their performance, operational status, and structural integrity. In the biomedical context, where the reliability and safety of devices are paramount, vibration order analysis is emerging as an essential tool to detect possible failures or anomalies.

This methodology can be applied to various medical devices, such as scanners, medical imaging devices, and infusion pumps. By understanding the characteristics of vibrations at specific frequencies, biomedical engineers can assess how well devices are functioning, anticipate potential problems, and implement preventative measures.

Analysis of the order of vibration signals in biomedical engineering also contributes to the development of safer and more effective medical devices. By identifying characteristic frequencies linked to specific phenomena, it is possible to optimize the device design and minimize unwanted vibrations.

A motor speed signal commonly consists of a sequence of tachometer pulses. Tachorpm function can be used to extract revolutions per minute (RPM) from a tachometer pulse signal. Tachorpm automatically identifies the pulse locations of a bilevel tachometer waveform and computes the interval between pulses to estimate rotational speed. In this example, the motor speed signal contains the rotational speed in rpm, and hence no conversion is needed. See **Figure 1** and **Figure 2** for the motor speed and vibration data as functions of time.

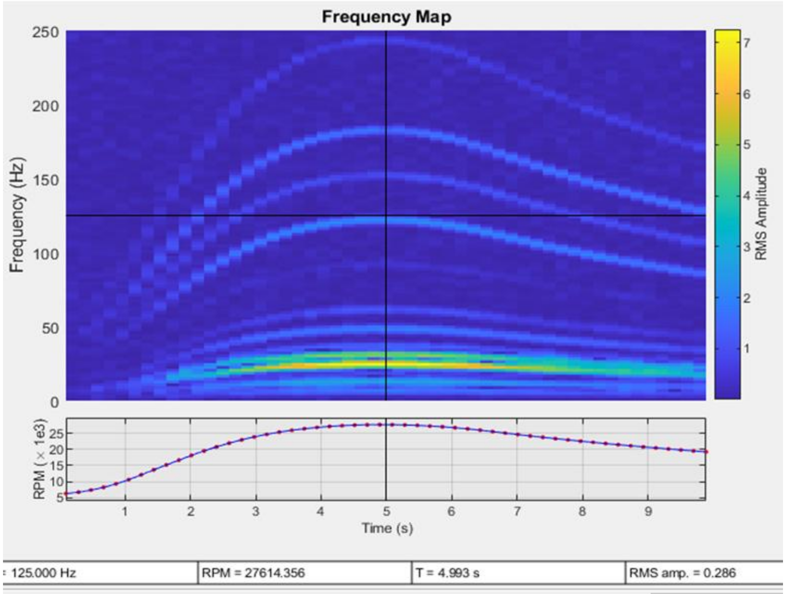

Figure 3. RPM-frequency map for vibration data. RPM: revolutions per minute.

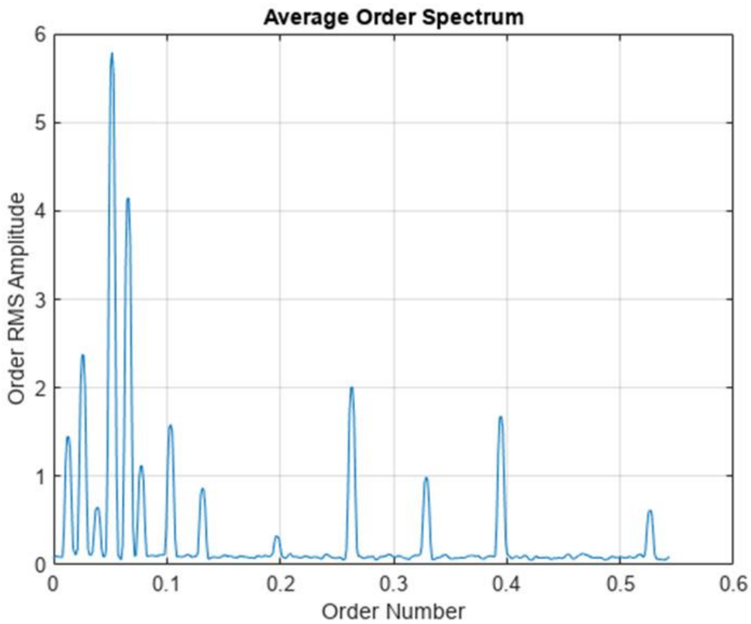

Figure 4. The average spectrum of map.

Figure 1 illustrates the variation in motor speed over time. The x-axis represents time, measured in seconds, depending on the duration of the data collection period. The y-axis represents motor speed, typically measured in RPM. The plot depicts how the motor speed changes throughout the recorded period. The trajectory of the curve provides insights into the motor's performance, behavior, and response to different conditions or stimuli.

Figure 2 illustrates the vibration data captured by an accelerometer over a specific duration of time. The x-axis represents time, typically measured in seconds, depending on the duration of the data collection period. The y-axis represents the accelerometer's vibration data, typically measured in units such as acceleration (m/s^2). The plot visually depicts how the vibration levels change over time, providing valuable insights into the dynamic behavior of the system being monitored. The trajectory of the curve reveals various characteristics of the vibration signal, which can be analyzed to assess the condition, performance, and health of machinery or structures.

Indeed, when analyzing vibration in rotating machinery, it is common to consider the changes in vibration amplitude as a function of rotational speed. The RPM profile, which corresponds to the engine speed during the run-up and coast-down phases, is a crucial parameter in vibration analysis.

Understanding the RPM profile and its influence on vibration amplitudes is crucial in vibration analysis. This knowledge allows the analysis and interpretation of vibration signals in the context of the machine's operational conditions and speed variations.

By considering the engine speed and its relationship to vibration characteristics, analysts can distinguish between normal operating conditions and potential faults or irregularities. This analysis approach aids in identifying specific frequencies associated with faults, detecting resonance effects, understanding gear, and bearing behavior, and diagnosing potential issues occurring at specific rotational speeds.

Visualizing data using an RPM-frequency map

The innovative approach to vibration analysis, utilizing an RPM-frequency map, exemplifies the intersection of data science and machinery diagnostics. By providing a visual narrative of the vibrational landscape, this technique enhances the precision and efficiency of maintenance practices, contributing to overall reliability and performance optimization.

Visualizing the vibration data using an RPM-frequency map facilitates the identification of potential dysfunction areas and aids in the diagnosis of rotating machinery. It provides a comprehensive overview of the vibration behavior of machinery across different RPM ranges, facilitating effective decision-making for maintenance, optimization, and ensuring reliable machinery operation (**Figure 3**).

Determining peak orders using an average order spectrum

Vibration analysis is a pivotal tool in predictive maintenance, allowing for the early detection of potential issues in machinery. An advanced technique in this domain involves the determination of peak orders using an average order spectrum, providing a nuanced understanding of the dynamic behavior of rotating equipment.

By determining peak orders using an average order spectrum (**Figure 4**), analysts can identify dominant frequency components associated with specific rotation orders, such as gear meshing frequencies or bearing fault frequencies. This provides essential information for diagnosing faults, assessing the condition of rotating machinery and optimizing operational parameters. Additionally, combining mid-order spectrum with other diagnostic techniques, such as envelope analysis or trend analysis, can improve fault detection and health monitoring capabilities. It involves calculating the average power spectral density or amplitude spectrum from multiple measurements. This averaging helps reduce the impact of random noise and highlights consistent frequency components.

In vibration analysis, maps can be used to show the relationship between different parameters, such as frequency and amplitude, in a spatial arrangement.

Conclusion

In conclusion, the analysis of the order of a vibration signal is emerging as an invaluable method in the field of biomedical engineering, especially in medical devices assisted diagnosis. This approach explores and interpret vibration characteristics in detail, thus providing significant advantages for the maintenance, reliability, and safety of medical devices.

Using order analysis, biomedical engineers can not only detect anomalies and potential failures but also anticipate emerging issues before they compromise device integrity or performance. This methodology provides an in-depth understanding of the specific frequencies associated with different phenomena, thereby facilitating the optimal design of safer and more effective medical devices.

References

[1] Ghemari Z. Progression of the vibratory analysis technique by improving the piezoelectric sensor measurement accuracy. Microw Opt Technol Lett 2018;60:2972-2977.

[2] Ghemari Z, Salah S, Bourenane R. Resonance Effect Decrease and Accuracy Increase of Piezoelectric Accelerometer Measurement by Appropriate Choice of Frequency Range. Shock Vib 2018;2018:5370438.

[3] Zhan C, Ji S, Liu Y, et al. Winding Mechanical Fault Diagnosis Technique of Power Transformer Based on Time-Frequency Vibration Analysis. 2018 Condition Monitoring and Diagnosis (CMD) 2018;1-6.

[4] Noubissi RK, Daosheng L, Boxue D. Study on Harmonic Response Analysis and Vibration Reduction of Amorphous Metal Alloy Transformer. 2023 IEEE 4th International Conference on Electrical Materials and Power Equipment (ICEMPE) 2023;1-4.

[5] Defdaf M, Ghemari Z, Elias Hadjaj A, et al. Improvement of Method Queues by Progress of the Piezoresistive Accelerometer Parameters. J Adv Manuf Syst 2017;16:227-235.

[6] Ghemari Z, Saad S. Parameters improvement and suggestion of new design of capacitive accelerometer. Analog Integr Circuits Signal Process 2017;92:443-451.

[7] Ghemari Z, Salah S. Simulation and Experimental Validation of New Model for the Piezoresistive Accelerometer Displacement. Sens Lett 2017;15:132–136.

[8] Ghemari Z, Belkhiri S, Saad S. Improvement of the Relative Sensitivity for Obtaining a High Performance Piezoelectric Sensor. IEEE Instrum Meas Mag 2023;26:49-56.

[9] Ghemari Z, Belkhiri S, Saad S. A capacitive sensor with high measurement accuracy and low electrical energy consumption. Appl Phys A 2023;129:362.

[10] Ghemari Z, Salah S, Defdaf M. Appropriate Choice of Damping Rate and Frequency Margin for Improvement of the Piezoelectric Sensor Measurement Accuracy. J Adv Manuf Syst 2021;1-12.

[11] Li C, Li J, Fang XL, et al. Application of a Method of Identifiying Instantaneous Shaft Speed from Spectrum in Aeroengine

Vibration Analysis. 2022 Global Reliability and Prognostics and Health Management (PHM-Yantai) 2022;1-7.
[12] Khatri P, Chhatre U, Kadge S. Visual Vibration Analysis of Vibrating Object at Low Frequency. 2021 6th International Conference for Convergence in Technology (I2CT) 2021;1-5.
[13] Belkhiri S, Ghemari Z, Saad S, et al. Improvement of the Vibratory Analysis by Enhancement of Accelerometer Characteristics. Sens Lett 2020;18:39-42.
[14] Ghemari Z, Saad S. Defects Diagnosis by Vibration Analysis and Improvement of Vibration Sensor Measurement Accuracy. Sens Lett 2019;17:608-613.
[15] Ghemari Z, Saad S, Khettab K. Improvement of the Vibratory Diagnostic Method by Evolution of the Piezoelectric Sensor Performances. Int J Precis Eng Manuf 2019;20:1361-1369.
[16] Ghemari Z, Saad S. Enhancement of capacitive accelerometer operation by parameters improvement. Int J Numer Modell: Electron Networks, Devices Fields 2019;32:e2568.
[17] Cao H, Huang T, Lu L, et al. Research on Quasi-zero Stiffness Vibration Isolation Technology of Distribution Transformer. 2021 IEEE 4th International Conference on Automation, Electronics and Electrical Engineering (AUTEEE) 2021;613-617.
[18] Tian Y, An T, Qin F, et al. Stress analysis of automotive IGBT module under vibration load. 2022 23rd International Conference on Electronic Packaging Technology (ICEPT) 2022;1-4.
[19] Coronado LOB, Ballesteros LIM, Geraldo EJT, et al. Finite Element Modal Analysis and Harmonic Response Analysis of a 3D Printed Vibration Sensor Enclosure. 2021 IEEE 13th International Conference on Humanoid, Nanotechnology, Information Technology, Communication and Control, Environment, and Management (HNICEM) 2021;1-5.
[20] Ghemari Z, Chouaf F, Saad S. New Formula for the Piezoresistive Accelerometer Motion Acceleration and Experimental Validation. J Adv Manuf Syst 2017;16:57-65.
[21] Balabanov IP, Mogilevets VD, Shabaev AA. Influence of Natural Vibration Frequencies in the Analysis on Vibration Resistance of Steel Supporting Parts of a Car. 2022 International Russian Automation Conference (RusAutoCon) 2022;448-452.
[22] Wang Y, Zhang H, Ji Y, et al. Micro-Vibration Prediction and Evaluation Analysis of the Structural Foundation of a Precision Instrument Plant Across the Reservoir. 2022 8th International Conference on Hydraulic and Civil Engineering: Deep Space Intelligent Development and Utilization Forum (ICHCE) 2022;1287-1291.
[23] Liu T, Cheng YJ, Li CF, et al. Research on correlation between modal and vibration of EMU bogie. 2021 4th International Conference on Electron Device and Mechanical Engineering (ICEDME) 2021;189-195.
[24] Yu Z, Li D, Chen L. Statistical analysis of vibration characteristics of power transformers with different voltage levels. 2018 12th International Conference on the Properties and Applications of Dielectric Materials (ICPADM) 2018;694-699.
[25] Liu D, Cai C, Wei B, et al. Investigation on the AMDT Core Model Vibration by Harmonic Response Analysis and Validation of the Resonance Characteristics by Testing. 2020 8th International Conference on Condition Monitoring and Diagnosis (CMD) 2020;43-46.
[26] Jiang X, Shang X, Jiang Y. Characteristic Analysis and Optimization Strategy of Transformer Vibration Signal. 2022 IEEE International Conference on Power Systems Technology (POWERCON) 2022;1-5.
[27] Wang S, Zhang H, Liu M, et al. Ice-induced vibration and fatigue analysis on monopile foundation of offshore wind turbine. 2022 IEEE International Conference on Advances in Electrical Engineering and Computer Applications (AEECA) 2022;1526-1531.
[28] Chao J, Ruihong J, Wen H, et al. Comparative Experiments of Optical Fiber Sensor and Piezoelectric Sensor based on Vibration Detection. 2020 IEEE 4th International Conference on Frontiers of Sensors Technologies (ICFST) 2020;17-20.
[29] Maga D, Hrad J, Hajek J, et al. FE Analysis of a Vibration Measuring Stand for Energy Harvester. 2020 19th International Conference on Mechatronics - Mechatronika (ME) 2020;1-4.
[30] Yang YN, Wang Q. Analysis of Vibration Noise and Transmission Characteristics of Flow-induced Rudder. 2021 OES China Ocean Acoustics (COA) 2021;456-459.
[31] Lin Y, Zhang J, Huang D. Study on Vibration Reduction Indicator of Metal Bellows Using Finite Element Analysis. 2021 IEEE 12th International Conference on Mechanical and Intelligent Manufacturing Technologies (ICMIMT) 2021;91-95.
[32] Song H, Song E, Liu Y, et al. Miniature FBG Vibration Sensor With High Performance and Low Angle Dependence for Two-Dimensional Vibration Measurement. IEEE Trans Instrum Meas 2023;72:1-11.
[33] Zhong L, Gao M, Zhou D, et al. Simulation Analysis of Mechanical Performance of 500kV Transformer Ascending Flanged Base

Under Vibration Excitation. 2023 IEEE 6th International Electrical and Energy Conference (CIEEC) 2023;3061-3065.
[34] Ghemari Z. Decrease of the resonance phenomenon effect and progress of the piezoelectric sensor correctness. 2018 International Conference on Electrical Sciences and Technologies in Maghreb (CISTEM) 2018;1-5.
[35] Ghemari Z. Analysis and optimization of vibration sensor. 2018 IEEE International Conference on Smart Materials and Spectroscopy (SMS) 2018;1-5.
[36] Linessio RP, Silva JCCd, Tavares LHdS, et al. Vibration analysis of a cantilever beam with viscoelastic neutralizers using fiber Bragg gratings. 2017 SBMO/IEEE MTT-S International Microwave and Optoelectronics Conference (IMOC) 2017;1-5.
[37] Fang XY, Li XY, Hu KM, et al. Destructive Reliability Analysis of Electromagnetic MEMS Micromirror Under Vibration Environment. IEEE J Sel Top Quantum Electron 2022;28:1-8.
[38] Aswin F, Suzen ZS. Analysis of free vibration measurement by mems accelerometer device on wind turbine blade. 2018 International Conference on Applied Science and Technology (iCAST) 2018;425-431.
[39] Das S, Rahman MW, Roy D, et al. Investigation on the Vibration of a 3-Phase SRM Analysis. 2022 IEEE 1st Industrial Electronics Society Annual On-Line Conference (ONCON) 2022;1-6.
[40] Zhang LF, Jiang BS, Zhang PQ, et al. Random Vibration Fatigue Analysis of Base In Macro-micro Motion Platform. 2021 Global Reliability and Prognostics and Health Management (PHM-Nanjing) 2021;1-6.
[41] Ghemari Z. Improvement of the piezoelectric sensor by the progress of the measurement accuracy. 2018 IEEE International Conference on Smart Materials and Spectroscopy 2018;1-5.
[42] Ghemari Z. Enhancement of the vibratory analysis technique by the accelerometer characteristics evolution. The 7th International Conference on Control Engineering & Information Technology 2019;1-4.
[43] Ghemari Z, Belkhiri S, Morakchi MR. Improvement of the vibration analysis technique by optimizing the parameters of the piezoelectric accelerometer. 2022 IEEE 21st international Conference on Sciences and Techniques of Automatic Control and Computer Engineering (STA) 2022;183-186.

Progress in Medical Devices
eISSN: 2957-5478

Zentime

Review Article https://doi.org/10.61189/620211pybxcq

Application of electrosurgery in gastrointestinal endoscopy

Hongrui Wang, Jiuzhou Zhao, Yu Zhou

School of Health Sciences and Engineering, University of Shanghai for Science and Technology, Shanghai 200093, China.

Corresponding authors: Yu Zhou.

Declaration of conflict of interest: None.

Received November 28, 2023; Accepted January 8, 2024; Published March 31, 2024

Highlights

- Proper parameter settings and mode selection are vital to minimize postoperative complications.
- Third Space Endoscopy offers innovative avenues beyond traditional methods for minimally invasive interventions.

Abstract

With the continuous advancement in medical device technology, minimally invasive surgery has become the cornerstone of modern surgical practices. At the forefront of this evolution is the fusion of medical endoscopes with high-frequency electrosurgical instruments, now a mainstream approach in minimally invasive surgeries, driving the development of innovative surgical procedures. This paper aims to provide an in-depth understanding of the principles of electrosurgical units, with a particular focus on standard procedures in gastrointestinal endoscopic electrosurgery. The goal of this review is to provide a more profound and comprehensive insight into endoscopic electrosurgery for medical practitioners and patients. Through the comprehensive study, it is anticipated to serve as a guide and reference for improving surgical outcomes, reducing patient discomfort, and simplifying the tasks of healthcare professionals.

Keywords: Electrosurgery, gastrointestinal endoscopy, clinical application

Introduction

High-frequency electric knife, with advantages such as rapid cutting speed, effective hemostasis, and convenient operation, notably simplifies surgical procedures for medical personnel and minimizes patient discomfort. Widely employed in various surgical disciplines, including general surgery, thoracic surgery, urology, otorhinolaryngology, cardiovascular surgery, gynecology, plastic surgery, orthopedics, and neurosurgery, the high-frequency electric knife has become an indispensable tool in surgical interventions. With the continuous progress of medical instruments, minimally invasive medicine has become pivotal in modern surgical practices. The integration of medical endoscopes with high-frequency electric knives, equipped with both cutting and coagulation capabilities, has become a prevalent approach in minimally invasive endoscopic surgeries, fostering the development of novel surgical techniques. However, many endoscopists lack comprehensive training and understanding of electrosurgical equipment. Therefore, this paper aims to enhance the knowledge and proficiency in managing electrosurgical units (ESUs) by introducing the principles of electrosurgery, associated equipment, and application of electrosurgery in gastrointestinal endoscopy.

Development of electrosurgery

The development of high-frequency electric knife is intricately linked with the discovery and evolution of electricity, as well as the profound exploration of electro-medicine by scholars throughout history. Goldwyn categorized the foundational epochs of electro-medicine into three significant historical periods leading up to

Address correspondence to: Yu Zhou, School of Health Sciences and Engineering, University of Shanghai for Science and Technology, No.516 Jungong Road, Shanghai 200093, China. Tel: 18021042556. E-mail: zhouyu@usst.edu.cn.

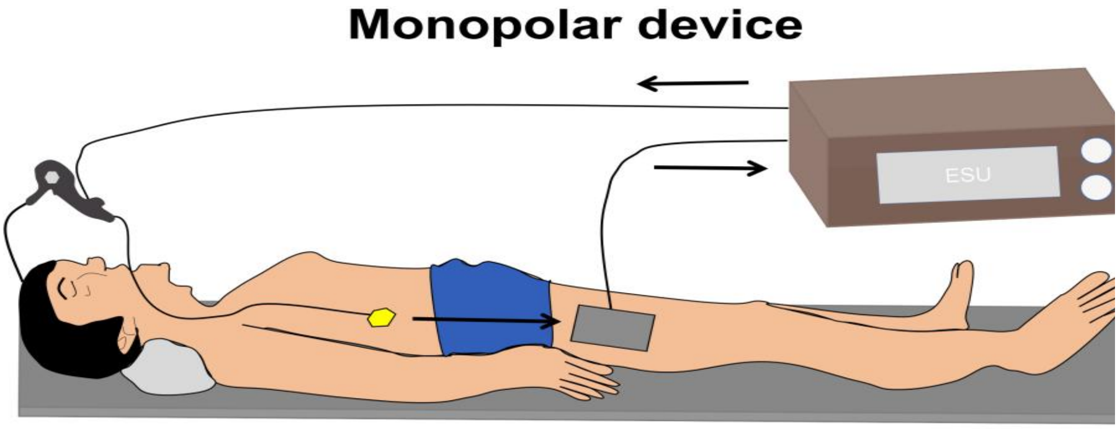

Figure 1. Monopolar device circuit. ESU, electrosurgical unit.

the introduction of the high-frequency electric knife [1]. The first epoch commenced with the discovery of static electricity, wherein static electricity was emerged as recognized as the only known form of electricity [2]. The second epoch, starting in 1786, was marked by Luigi Galvani's observation that frogs' legs spasm upon contact with different metals, introducing the concept of "animal electricity" [3]. In 1800, Volta et al. invented the "Voltaic pile", confirming that continuous electrical stimulation could induce sustained muscle contractions, laying the groundwork for electro-medicine [4]. The third epoch can be traced back to 1831, when Michael and Joseph independently discovered the phenomenon of "electromagnetic induction", a breakthrough that significantly accelerated development of electro-medicine [5].

The precursor to the high-frequency electric knife emerged in the late 19th and early 20th centuries. In 1891, Jacques discovered that high-frequency electrical currents above 100 kHz passing through the human body did not cause pain but elevated the temperature [6]. This breakthrough paved the way for electrosurgical technology. In 1900, Joseph, while treating a patient with high-frequency electric current, accidentally discovered that the electric arc generated by the electrode could coagulate the skin [7]. Subsequently, he successfully treated a patient with a hand ulcer using this electric arc current [7]. This event is considered the birth of electrosurgery. In 1926, Harvey performed the world's first electrosurgical procedure using an electric knife manufactured by William, ushering in the era of electrosurgery [8].

Early high-frequency electric knives primarily utilized spark gap discharge mechanisms, relying on capacitors, inductors, and adjustable spark electrodes. They generated arc sparks through high alternating current voltage, posing a significant risk of burn accidents and carrying substantial inherent risks [9]. With the development of semiconductor technology, high-frequency electric knife devices gradually transitioned to utilizing semiconductor technologies such as transistors and metal-oxide-semiconductor field-effect transistors, coupled with high-frequency sinusoidal waves with lower harmonic components as the output waveform. Simultaneously, high-performance microprocessors were employed for control, enhancing the precision and safety of equipment control [10, 11].

Today, high-frequency electric knives find widespread application across various surgical disciplines. With the deepening of the concept of minimally invasive surgery, high-frequency electric knives are also commonly used in endoscopic procedures. For example, VIO series electrosurgical devices manufactured by ERBE Elektromedizin GmbH utilize Hybrid Knife technology, enabling various digestive surgical procedures in conjunction with endoscopy [12]. In contrast to traditional open surgy for gastrointestinal disorders, which are characterized by minimal patient trauma, thorough curative outcomes, and lower treatment costs. These procedures have evolved into the primary therapeutic modality for early gastrointestinal diseases on an international scale in recent years.

Principles of electrosurgery

Electrosurgery utilizes electrical energy to generate heat effects for medical purposes, such as excision, incision, hemostasis, and inactivation of target tissues. The therapeutic foundation of all electrosurgical procedures lies at the cellular level, where heat effects are induced. When high frequency alternating current, generated by ESUs, flows through tissues along the circuit, it encounters resistance which generates heat [13]. Specifically, within

Table 1. The thermal effect of human tissue

Temperature	Effect
≤40 °C	No effect.
40-50 °C	Cell membrane and intracellular structures change depend on the duration of heating.
50-60 °C	Coagulation (denaturation) of cellular proteins; Loss of viability.
60-80 °C	Coagulation of extracellular collagen; Disruption of cell membrane.
80-100 °C	Vaporization of tissue fluid; Desiccation and damage to cells; Tissue rupture resulting in incisions.
>150 °C	Carbonization.
>300 °C	Evaporation.

the circuit of high-frequency alternating current, the anions and cations within the tissue migrate towards positions near the positive and negative poles, respectively, based on the current-voltage direction. As the polarity rapidly changes, the movement direction of anions and cations within the tissue also changes swiftly. These particles oscillate rapidly within the cytoplasm, converting electrical energy into mechanical energy and, through friction, ultimately transforming into heat energy, resulting in a thermal effect [14]. These effects are primarily determined by the temperatures achieved, as outlined in **Table 1**. The most crucial effect of electrosurgical procedures is the denaturation of proteins, varying from coagulation at 60 °C to evaporation at 100 °C. The speed and extent of these processes depend on the heating rate and effective duration of temperature elevation [15].

ESUs, which generate electrosurgical energy, can be categorized into monopolar and bipolar devices, based on the current path. Monopolar technology is defined as high-frequency electric current flowing to the active electrode towards the target tissue, then returning through the body to the neutral grounding pad, ultimately forming a circuit, as shown in **Figure 1**. The current intensity (I) is defined as the ratio of the quantity of charge (q) through a conductor's cross-section to time (t), mathematically expressed as $I=q/t$. Current intensity is a physical quantity that describes the strength of the current at a specific point in an electrical circuit, representing the amount of current passing through a unit cross-sectional area. Current intensity is directly proportional to voltage (U) and inversely proportional to resistance (R). A higher working voltage leads to greater current intensity, while higher resistance results in lower current intensity [16]. Therefore, smaller tissue surfaces in contact with the active electrode generate higher current intensity, producing more significant thermal effects. In contrast, the contact area with the neutral grounding pad, which is well in contact with the body compared to the active electrode, has a larger surface area, making the thermal effects negligible. However, if there is poor contact with the neutral grounding pad, localized temperature elevation may occur, potentially causing skin burns. Thus, operators should be cautious in such cases. Bipolar technology involves high-frequency electric current emanating from one pole of the bipolar electrode, passing through nearby tissue to reach the other pole and then returning to the ESU, completing a circuit, as illustrated in **Figure 2**. The advantages of bipolar technology include the reduced travel distance of current within the body, limited thermal damage, and the ability to achieve similar effects with lower power, thereby reducing the risk of perforations [17]. Most ESUs used in digestive endoscopy support both monopolar and bipolar modes. However, monopolar mode is preferred due to its compatibility with a wider range of surgical instruments, facilitating both cutting and coagulation. On the other hand, bipolar mode instruments are generally less available and mainly designed for coagulation, with only a select few intended for cutting. Currently, despite the development of instruments suitable for bipolar mode, such as polypectomy snares, thermal biopsy forceps, sphincterotomes, IT knives and others, their widespread use remains limited [18-20]. This is partly due to their higher design and manufacturing costs compared to monopolar instruments. In summary, it is essential for endoscopists to have a thorough understanding of the characteristics of the instruments they choose to reduce the risk of accidents.

In addition to device types, the output waveform mode is also crucial. ESUs are designed to offer operators various output waveform modes labeled as "Cut", "Blend", "Coag" and others. It's important to note that these names are not standardized, and modes may vary with the same name between ESUs produced by different companies [21]. Endoscopists should

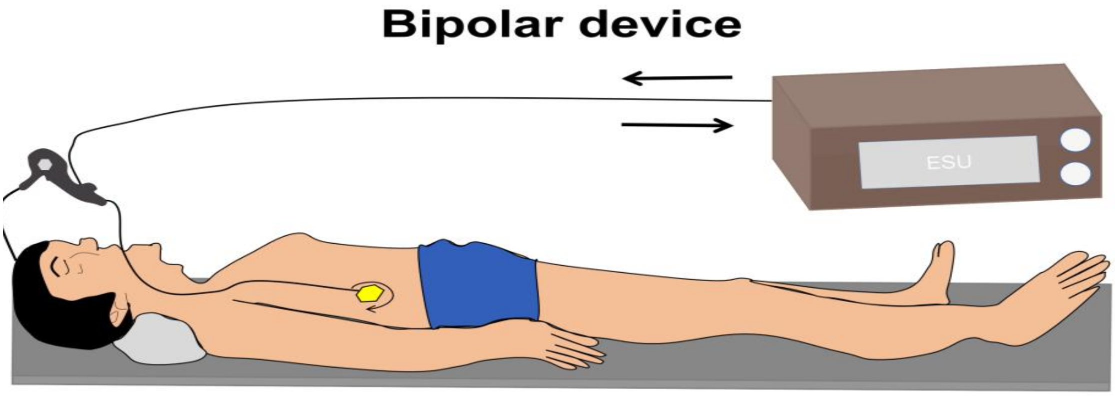

Figure 2. Bipolar device circuit. ESU, electrosurgical unit.

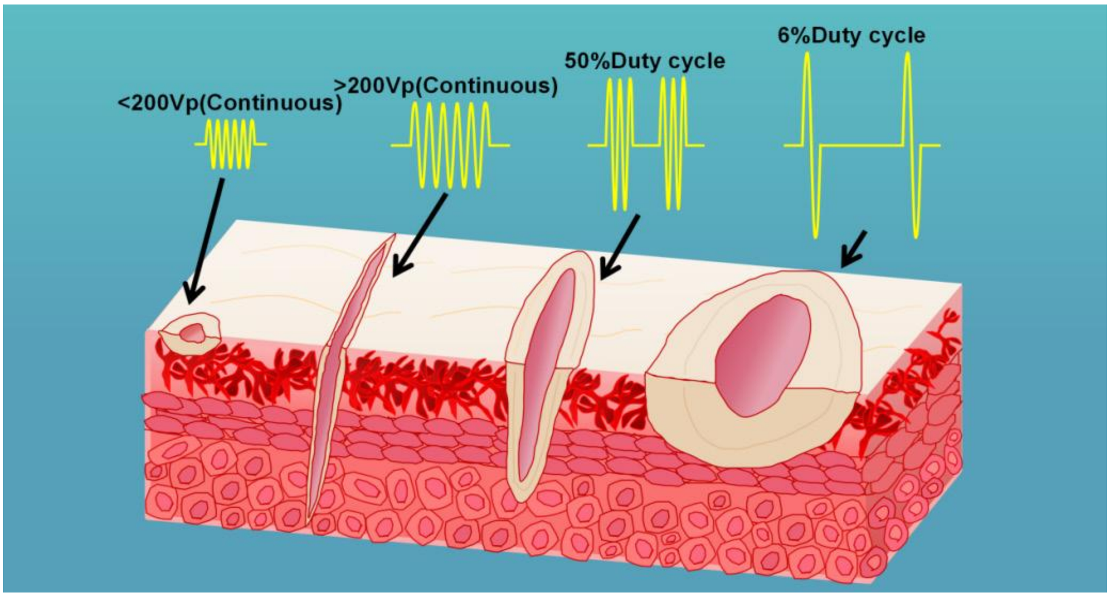

Figure 3. The effect of different waveforms.

carefully read the user manual of devices prior to operation. A profound understanding of the selected output waveform is crucial, as mode names can sometimes be misleading. For example, many outputs labeled as "Coag" can produce significant cutting capabilities. Pure coagulation effects can only be achieved with waveforms where the voltage peak does not exceed 200 V, commonly known as "Soft Coag" [22]. ESUs typically produce output ranging from continuous low-frequency sine waves to modulated interrupted higher-frequency sine waves, as illustrated in **Figure 3**. When the voltage peak of continuous waveforms exceeds 200 V, it rapidly generates high current density along the electrode, which creates a significant amount of heat, causing cell explosions, and results in a cutting effect. Cells farther from the electrode do not receive enough heat to explode, leading to coagulation. Even in modes labeled as "Pure Cut," there may be some coagulation along the cutting edge. Accurate "Pure Cut" is achieved only with cold-cutting instruments like surgical knives. When using an electrosurgical knife at voltages exceeding 200 V, the coagulation depth along the cutting-edge increases. However, it is impractical to endlessly boosting voltage for more coagulation, especially beyond about 600 V peak voltage due to excessive power [10]. The released heat (Q), calculated using Joule's law, is the product of power and time (Q=W×t). By combining Ohm's law in this equation ($Q=V\times I\times t=I^2\times R\times t$), there is a risk of carbonization on cutting surfaces [22]. Intermittently halting the output allows tissue cooling, increasing the proportion of cells that dry without exploding. By adjusting the duty cycle and applying higher voltage peaks in the output, the coagulation edge of the tissue can be enhanced, achieving a deeper hemostatic effect. These modulated waveforms are termed "Blend" and "Coag." Typically, coagulation waveforms have a lower duty cycle, ranging between 6% and 12%, while blend waveforms have a duty cycle between 12% and 80% [23]. "Crest factor" is another concept when discussing waveforms and is often found in the ESU product manuals. It refers to the ratio of the current peak value to the effective current value on the load. For instance, the crest factor

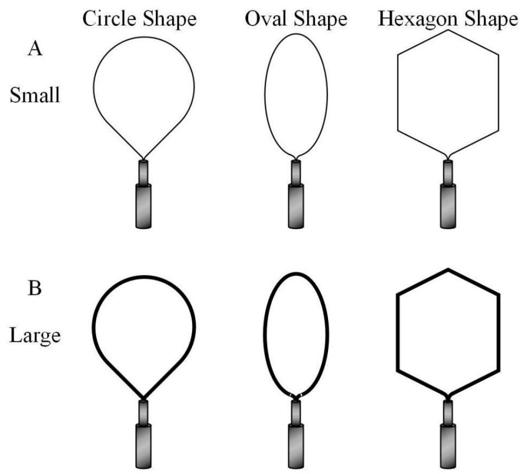

Figure 4. Different shapes and sizes of snares. (A) Small size snares; (B) Large size snares.

for a continuous sine wave is 1.4. Generally, cutting waveforms are characterized by crest factors less than 2, while blend waveforms have crest factors ranging between 2 and 5 and coagulation waveforms have crest factors ranging between 5 and 8 [22]. Endoscopists should understand the electrophysiological characteristics produced by different waveform modes and choose the most appropriate mode based on practical application scenarios.

Application of electrosurgery in gastrointestinal endoscopy

Endoscopic surgery has emerged as a safe and effective method for treating early gastrointestinal lesions, replacing traditional open surgery as a routine endoscopic treatment method [24]. The Paris endoscopic classification now plays a pivotal role in clinical practice, serving as the gold standard for endoscopic and visual assessment of gastrointestinal lesions [25]. In clinical practice, the Paris classification is widely employed to determine the type of lesion for subsequent selection of resection methods based on the size, location, and pathological diagnosis of the lesion. Gastrointestinal polyps are the most prevalent lesions encountered in clinical practice. Given the risk of malignancy associated with these lesions, early diagnosis and treatment are crucial. Endoscopic treatment for gastrointestinal polyps often employs various electrocautery techniques, such as hot snare polypectomy (HSP), argon plasma coagulation (APC), endoscopic mucosal resection (EMR), and endoscopic submucosal dissection (ESD). Additionally, the growing experience in endoscopic surgery and technological advancement has led to the development of a new technique that creates a submucosal tunnel, introducing a novel domain known as "third space endoscopy" for treating gastrointestinal ailments. One representative procedure of this frontier technology is peroral endoscopic myotomy (POEM) for esophageal sphincter myotomy.

HSP

Depending on the type of electrosurgical devices, polypectomy is divided into cold snare polypectomy (CSP) and HSP. CSP is generally effective for polyps measuring 3-5mm in diameter [26, 27]. It offers a shorter operating time and lower risk of thermal injury to the intestinal wall [28]. For polyps measuring 5-10mm, both methods have pros and cons, with CSP having a higher risk of incomplete resection [29]. For polyps of 10-19 mm, the European Society of Gastrointestinal Endoscopy recommends using HSP technology [30]. Compared to CSP, the cauterization effect of HSP may extend to the submucosal layer, making it more suitable for deep and complete removal of larger polyps. Submucosal preventive injection of normal saline, adrenaline, or other mixtures is recommended before HSP to reduce the risk of bleeding and prevent deep colonic mucosal thermal injury [30-32]. The HSP procedure involves positioning the hot snare into the biopsy channel, completely snaring the polyp, gradually tightening the snare, and subsequently connecting the electrosurgical energy-generating device to the snare for complete resection. Doctors need to choose the appropriate snare instrument based on the size and shape of the lesion. Commonly used snare instruments include circular, oval, hexagonal, etc., as illustrated in **Figure 4**. It's crucial to recognize that the choice of snare affects the current density and the nature of the cut: a thinner-edged snare yields a higher current density for precise cutting, whereas a thicker-edged snare offers lower current density, favoring coagulation. Currently, the Blend mode is the preferred option during the HSP process. A pure cutting mode may elevate the risk of transient bleeding with limited hemostatic effects. In contrast, a coagulation mode may increase the potential for transmural damage to the intestinal wall due to its deeper action, leading to electrosurgical syndrome [33]. Therefore, the Blend mode, which has a cutting effect at the excision site and a coagulation effect at the excision edge, represents the most suitable choice.

APC

APC is a non-contact tissue coagulation technique that utilizes argon gas discharge under atmospheric pressure to coagulate tissue without requiring the tissue to adhere to the electrode. Its application in electrosurgery is

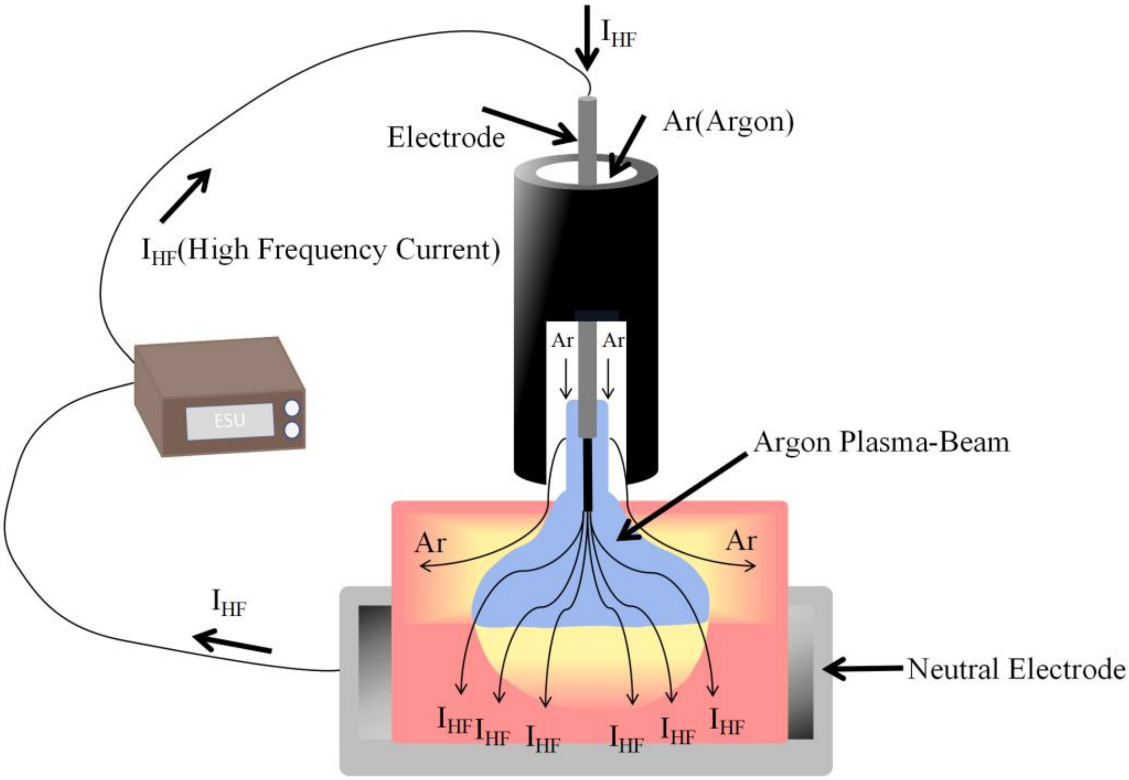

Figure 5. The fundamental working process of argon plasma coagulation.

widespread. Initially introduced in open surgical procedures in the late 1970s, APC found its endoscopic application in 1991, quickly becoming the preferred endoscopic coagulation technique [34, 35]. Argon gas was chosen due to its biochemical inertness, low breakdown voltage, and relatively low cost [36]. The principle of operation involves the transmission of electrical energy to the target tissue through an ionized argon plasma jet. The basic working process is illustrated in **Figure 5**. As tissue conductivity decreases and resistance increases, the argon plasma will automatically shift from the high resistance zone to the low resistance zone. The penetration depth of coagulation is limited to a few millimeters. Compared to other endoscopic thermal coagulation methods, APC provides quick hemostasis, minimal bleeding, and reduced scab formation. Typically, APC can be used as an adjunctive treatment for gastrointestinal polyps, effectively reducing postoperative residual tissue. Brooker et al. evaluated the role of APC in preventing recurrence at the polypectomy sites and confirmed its safety and effectiveness [37]. In addition, this technique is also suitable for treating erosion, ulcers, polyps, tumors, and other superficial lesions of the digestive mucosa by halting bleeding, relieving pain, and mitigating inflammation. Hybrid APC is a relatively new technology in this field. It combines traditional APC with prior submucosal injection using water jet-assisted submucosal dissection, representing a development of APC technology [38]. Compared to standard APC, submucosal injection serves as a heat sink to disperse energy, ensuring that the underlying intrinsic muscle layer remains unaffected and only the intact mucosal layer is coagulated, providing better safety [39].

EMR

EMR is a minimally invasive endoscopic surgery developed by Japanese experts in the 1980s [40]. It aims to completely remove pathological mucosa by submucosal dissection. EMR surgery is mainly suitable for early cancer surgery and can also be extended to removal of polyps and resection of partial precancerous lesions, typically those smaller than 20 mm. The most used techniques can be further categorized as injection-assisted EMR, as shown in **Figure 6**, cap-assisted EMR, as shown in **Figure 7**, and ligation-assisted EMR, as shown in **Figure 8**.

Injection-assisted EMR

The initial step of this technique involves injecting a solution into the mucosa to lift it, making it easier to capture the lesion. The common injection substances include physiological saline, a combination of fibrinogen, sodium hyaluronate, hydroxypropyl methylcellulose, glycerol, or hydroxyethyl starch. This injection serves as a buffer zone between the lesion and normal tissue, minimizing damage to the deeper layers of gastrointestinal wall during electro-surgery. Staining agents can be mixed into the injection

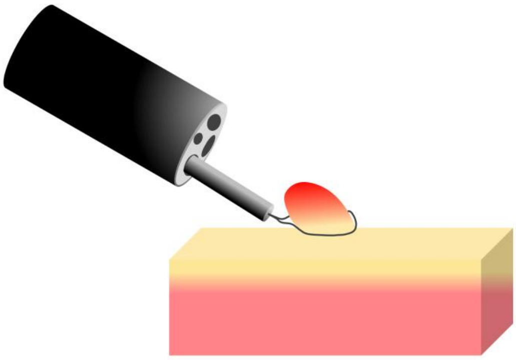

Figure 6. Injection-assisted endoscopic mucosal resection.

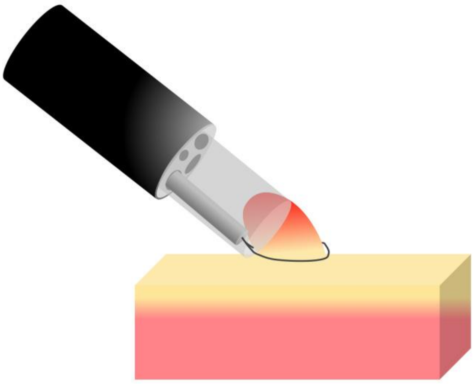

Figure 7. Cap-assisted endoscopic mucosal resection.

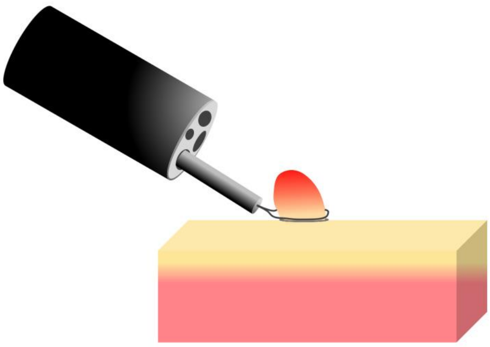

Figure 8. Ligation-assisted endoscopic mucosal resection.

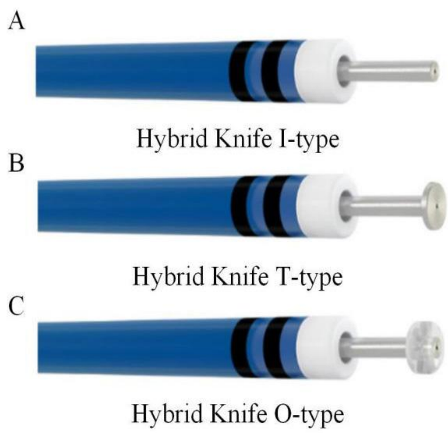

Figure 9. Hybrid Knife. (A) I-type; (B) T-type; (C) O-type. This figure was cited from the official website of Hybrid Knife (ERBE Elektromedizin GmbH).

material to identify the boundaries of the lesion more clearly [41]. Current research indicates that using autologous blood or adrenaline as injection materials can more effectively reduce the risk of bleeding and perforation [42, 43]. If the lesion cannot be effectively raised during injection, it may indicate deeper tissue invasion, and EMR should not be used for excision in such cases.

Cap-assisted EMR

This technique does not require submucosal injection. It involves using a cap-fitted endoscope to aspirate the lesion tissue, followed by excision using the electric surgery snare technique. The cap is typically made of transparent plastic, usually in a straight cylindrical shape or with an oblique pointed end. It can be either soft or hard, chosen based on the specific surgical site. Soft caps are commonly used in EMR procedures as they can reduce mucosal damage during surgery [44]. For gastric lesion surgeries, a straight cap is often used, while for esophageal lesion resection procedures, an oblique cap is commonly employed to compensate for the position and angle of the endoscope relative to the esophageal wall [45].

Ligation-assisted EMR

This technique does not require submucosal injection. Instead, it involves placing a variceal ligation band on the lesion tissue. Using suction, the lesion is pulled into the ligator. The contracting force squeezes the mucosa and submucosal layers without capturing the intrinsic muscle layer. Subsequently, the ligator is removed, and the lesion is excised using the electric surgery snare either above or below the ligated band [45].

ESD

ESD is an advanced technique for the endoscopic removal of mucosal lesions, offering a minimally invasive treatment for early gastrointestinal cancer lesions. Originating in Japan in the late 1990s as a treatment for early gastric cancer, ESD's applicability has expanded to include esophagus and colon lesions [46]. ESD offers advantages over EMR: notably its ability to excise larger lesions irrespective of their size, bringing about higher cure rates, lower recurrence rates, and precise histopathological analysis [47]. However, research indicates that EMR may be more advantageous for lesions (<10 mm) in size [48]. Currently, ESD has largely replaced EMR as the preferred surgical approach for early cancer surgeries worldwide, due to its growing prevalence and effective [49, 50]. The core steps of ESD involve lesion marking, submucosal injection to lift the lesion, dissecting, and achieving hemostasis. The technique employs a variety of specialized surgical knives, including the Dual Knife (Olympus), Flex Knife (Olympus), Flush Knife (Fujifilm), Hook Knife (Olympus), Triangle Tip Knife (Olympus), Hybrid Knife (ERBE Elektromedizin GmbH) and so on. Each knife has its own advantages, allowing for a rational selection based on lesion location and structural characteristics [51]. The Hybrid Knife from ERBE Elektromedizin GmbH is particularly advantageous as a multifunctional tool suitable for marking, excision, and submucosal injection. It significantly reduces the need for frequent instrument changes during surgery, thereby improving operational efficiency. Its integrated central capillary tube, when used in conjunction with the ERBEJET 2 system, can generate a 120 μm water jet for submucosal injection. The Hybrid Knife is available in three models: I-type, T-type, and O-type, as shown in **Figure 9**, offering greater flexibility in selection. **Figure 9** was cited from the official website of Hybrid Knife (ERBE Elektromedizin GmbH). Common ESU devices used in clinical endoscopic treatment include the ERBE VIO200S, VIO200D, VIO300S, and VIO300D series. Many other companies also offer similar ESU devices suitable for endoscopic treatment. However, regardless of the choice for ESU or knife, it is essential to adjust parameter settings flexibly based on the actual cutting and coagulation needs during surgery, in accordance with the clinician's experience, to achieve safe and effective surgery. Despite the absence of specific guidance on ESU settings for ESD surgery, a study by Masamichi Arao et al. regarding the use of the ENDO CUT mode and FORCED COAG mode of the VIO300D in pig esophageal endoscopic submucosal dissection demonstrated that the ENDO CUT mode significantly reduced the stricture rate and fibrosis degree compared to the FORCED COAG mode [52]. Additionally, Tonai et al. used the VIO300D to assess the effects of various modes on fibrosis and stricture in pig muscle layers after ESD, and found that among all ESU modes, the ENDO CUT mode exhibited the lowest stricture and fibrosis [53] . Therefore, it is recommended to minimize the use of the coagulation mode in regions prone to stricture formation, such as the esophagus, to reduce the occurrence of postoperative stricture-related complications.

POEM

In 1957, Hirschowitz developed the fiber optic scope, laying the groundwork for the invention of a stomach camera equipped with this technology that was subsequently widely adopted in Japan [54]. This innovation paved the way for endoscopy in the colon, esophagus, and duodenum [55]. The traditional endoscopic examination process, known as the first-space endoscopy, was conducted within the natural cavity of the gastrointestinal tract. In 2004, Kalloo et al. performed transoral intraperitoneal endoscopy in a porcine model, introducing the concept of second-space endoscopy [56]. In 2007, Sumiyama et al. first described the technique of using a mucosal flap valve to safely breach the gastrointestinal wall in a porcine model, known as submucosal tunneling technology [57]. Pasricha et al. further used this technique to successfully implement submucosal endoscopic myotomy in a porcine model [58]. Finally, in 2008, Inoue et al. performed the first case of POEM to treat achalasia, ushering in a new approach for third-space endoscopy treatment [59].

POEM, the first successful innovative technique in third-space endoscopy, has emerged as the preferred treatment for achalasia and other esophageal spastic disorders [60, 61]. The procedure involves several key steps: mucosal incision, submucosal dissection, myotomy, and mucosal closure [62]. When establishing the submucosal tunnel, it is essential to perform a thorough submucosal injection to ensure an excellent surgical field. Close attention should be paid to the condition of submucosal vessels to minimize bleeding. Prompt coagulation is necessary to maintain a clear view in case of bleeding. During POEM, a strong coagulation mode with high pressure and low duty cycle is typically used for small vessels or large capillaries. In contrast, a soft coagulation mode with <200 Vp continuous is used for significant vessels [63]. It is essential to wait for complete hemostasis before resuming cutting to ensure a clear surgical field. So far, there is limited data on the optimal mode and power settings of electrosurgical devices for endoscopic tunneling techniques, and research on this topic is still lacking. Parameter settings are mainly based on the equipment's actual conditions and endoscopists' personal experience, with common modes and power settings similar to those used in EMR and ESD [64].

Conclusions

Over the past 40 years, high-frequency electrosurgical technology has evolved and wide applied in digestive endoscopic examinations. In electrosurgical procedures, high-frequency electric current generates heat within tissues.

The various parameters of electrosurgical energy-generating devices, including current waveform, power, electrode type, and the specific device used, are closely associated with the occurrence of surgical complications. The parameter settings may vary significantly depending on the type of procedures. Therefore, it is essential for endoscopists to have an in-depth understanding of electrosurgical devices and their settings, which is critical to optimizing the safety and efficacy of a wide range of surgical interventions.

References

[1] Goldwyn RM. Bovie: the man and the machine. Ann Plast Surg 1979;2:135-153.

[2] Beard GM, Rockwell AD. A practical treatise on the medical and surgical uses of electricity: including localized and general electrization. New York : William Wood. Nabu Press, 1871. p.698.

[3] Galvani, Luigi. Commentary on Power in Sports. Typographia Instituti Scientiarum 1791;363-418.

[4] Alexander Volta. On the electricity excited by the mere contact of conducting substances of different kinds. Philos Trans of the R Society of Lon 1800;90(90):403-431.

[5] Cambridge NA. Electrical apparatus used in medicine before 1900. Proc R Soc Med 1977;70:635-641.

[6] WARD GE. Electrosurgery. Interne 1947;13(8): 347-351.

[7] Glover JL, Bendick PJ, Link WJ. The use of thermal knives in surgery: electrosurgery, lasers, plasma scalpel. Curr Probl Surg 1978; 15:1-78.

[8] Cushing H. Electro-surgery as an aid to the removal of intracranial tumors. Surg Gynecol Obstet 1928;47:751-755.

[9] Ha A, Richards C, Criman E, et al. The safe use of surgical energy devices by surgeons may be overestimated. Surg Endosc 2018;32:3861-3867.

[10] Morris ML, Tucker RD, Baron TH, et al. Electrosurgery in gastrointestinal endoscopy: principles to practice. Am J Gastroenterol 2009;104:1563-1574.

[11] Massarweh NN, Cosgriff N, Slakey DP. Electrosurgery: history, principles, and current and future uses. J Am Coll Surg 2006;202: 520-530.

[12] Kaehler GF, Sold MG, Lingenfelder T, et al. Needle Knife and Water Jet Combined As a Hybrid Knife-A Comparison with Standard Knife in An In Vivo Animal Study. Gastrointest Endosc 2007;65:AB285.

[13] Barlow DE. Endoscopic applications of electrosurgery: a review of basic principles. Gastrointest Endosc 1982;28:73-76.

[14] Malis LI. Electrosurgery. Technical note. J Neurosurg 1996;85:970-975.

[15] Carr-Locke, David L, John Day. Principles of Electrosurgery. ERCP 2011;11:125-134.

[16] Zinder DJ. Common myths about electrosurgery. Otolaryngol Head Neck Surg 2000; 123:450-455.

[17] Tucker RD, Sievert CE, Platz CE, et al. Bipolar electrosurgical sphincterotomy. Gastrointest Endosc 1992;38:113-117.

[18] Tucker RD, Platz CE, Sievert CE, et al. In vivo evaluation of monopolar versus bipolar electrosurgical polypectomy snares. Am J Gastroenterol 1990;85:1386-1390.

[19] Savides TJ, See JA, Jensen DM, et al. Randomized controlled study of injury in the canine right colon from simultaneous biopsy and coagulation with different hot biopsy forceps. Gastrointest Endosc 1995;42:573-578.

[20] Saito Y, Uraoka T, Matsuda T, et al. Endoscopic treatment of large superficial colorectal tumors: a case series of 200 endoscopic submucosal dissections (with video). Gastrointest Endosc 2007;66:966-973.

[21] Waye JD, Geenen J, Fleischer DF, et al. Techniques in therapeutic endoscopy. Pennsylvania: Philadelphia, Saunders, 1987. 1st edition.

[22] Marín-Gabriel JC, Romito R, Guarner-Argente C, et al. Use of electrosurgical units in the endoscopic resection of gastrointestinal tumors. Gastroenterol Hepatol 2019;42:512-523.

[23] Tokar JL, Barth BA, Banerjee S, et al. Electrosurgical generators. Gastrointest Endosc 2013;78:197-208.

[24] Swanström LL, Khajanchee Y, Abbas MA. Natural orifice transluminal endoscopic surgery: the future of gastrointestinal surgery. Perm J 2008;12:42-47.

[25] Fujiyoshi MRA, Inoue H, Fujiyoshi Y, et al. Endoscopic classifications of early gastric cancer: A literature review. Cancers (Basel) 2021;14:100.

[26] Karstensen JG, Ebigbo A, Desalegn H, et al. Colorectal polypectomy and endoscopic mucosal resection: European society of Gastrointest Endosc cascade guideline. Endosc Int Open 2022;10:E1427-E1433.

[27] Tanaka S, Saitoh Y, Matsuda T, et al. Evidence-based clinical practice guidelines for management of colorectal polyps. J Gastroenterol 2021;56:323-335.

[28] Kawamura T, Takeuchi Y, Asai S, et al. A comparison of the resection rate for cold and hot snare polypectomy for 4–9 mm colorectal polyps: a multicentre randomised controlled trial (CRESCENT study). Gut 2018;67:1950-

1957.
[29] Ito A, Suga T, Ota H, et al. Resection depth and layer of cold snare polypectomy versus endoscopic mucosal resection. J Gastroenterol 2018;53:1171-1178.
[30] Ferlitsch M, Moss A, Hassan C, et al. Colorectal polypectomy and endoscopic mucosal resection (EMR): European Society of Gastrointest Endosc (ESGE) clinical guideline. Endoscopy 2017;49:270-297.
[31] Feitoza AB, Gostout CJ, Burgart LJ, et al. Hydroxypropyl methylcellulose: a better submucosal fluid cushion for endoscopic mucosal resection. Gastrointest Endosc 2003;57:41-47.
[32] Dobrowolski S, Dobosz M, Babicki A, et al. Prophylactic submucosal saline–adrenaline injection in colonoscopic polypectomy: prospective randomized study. Surg Endosc 2004;18:990-993.
[33] Kim HS, Kim TI, Kim WH, et al. Risk Factors for Immediate Postpolypectomy Bleeding of the Colon: A Multicenter Study. Am J Gastroenterol. 2006;101(6):1333-1341.
[34] Morrison JC, inventor; MORRISON JR CHARLES F, assignee. Electrosurgical method and apparatus for initiating an electrical discharge in an inert gas flow. US patent US19760649682. 1976/01/16.
[35] Farin G, Grund K. Technology of argon plasma coagulation with particular regard to endoscopic applications. Endosc Surg Allied Technol 1994;2:71-77.
[36] Zenker M. Argon plasma coagulation. Argon plasma coagulation. GMS Krankenhhyg Interdiszip 2008;3(1):15.
[37] Brooker JC, Saunders BP, Shah SG, et al. Treatment with argon plasma coagulation reduces recurrence after piecemeal resection of large sessile colonic polyps: a randomized trial and recommendations. Gastrointest Endosc 2002;55:371-375.
[38] Manner H, Kouti I, May A. Efficacy and safety of hybrid-APC for the ablation of Barrett's esophagus. Surg Endosc 2016;30:1364-1370.
[39] Shah SN, Chehade NEH, Tavangar A, et al. Hybrid argon plasma coagulation in Barrett's esophagus: a systematic review and meta-analysis. Clin Endosc 2023;56:38-49.
[40] Tada M. A new technique of gastric biopsy. Stomach Intestine 1984;19:1107-1116.
[41] Hirao M, Masuda K, Asanuma T, et al. Endoscopic resection of early gastric cancer and other tumors with local injection of hypertonic saline-epinephrine. Gastrointest Endosc 1988;34:264-269.
[42] Sato T. A novel method of endoscopic mucosal resection assisted by submucosal injection of autologous blood (blood patch EMR). Dis Colon Rectum 2006;49:1636-1641.
[43] Tanaka M, Ono H, Hasuike N, et al. Endoscopic submucosal dissection of early gastric cancer. Digestion 2008;77:23-28.
[44] Desai PN, Patel CN, Kabrawala M, et al. Distal Endoscopic Attachments. J Dig Endosc 2022;13:243-250.
[45] Kantsevoy SV, Adler DG, Conway JD, et al. Endoscopic mucosal resection and endoscopic submucosal dissection. Gastrointest Endosc 2008;68:11-18.
[46] Makuuchi H, Shimada H, Mizutani K, et al. Endoscopic mucosal resection in early esophageal cancer. Nihon Kikan Shokudoka Gakkai Kaiho 1996;47:150-154.
[47] Pimentel-Nunes P, Pioche M, Albéniz E, et al. Curriculum for endoscopic submucosal dissection training in Europe: European Society of Gastrointest Endosc (ESGE) position statement. Endoscopy 2019;51:980-992.
[48] Han C, Sun Y. Efficacy and safety of endoscopic submucosal dissection versus endoscopic mucosal resection for superficial esophageal carcinoma: a systematic review and meta-analysis. Dis Esophagus 2021; 34:doaa081.
[49] Ma MX, Bourke MJ. Endoscopic submucosal dissection in the West: current status and future directions. Digestive Endoscopy 2018;30:310-320.
[50] Draganov PV, Wang AY, Othman MO, et al. AGA institute clinical practice update: endoscopic submucosal dissection in the United States. Clin Gastroenterol Hepatol 2019;17:16-25.e1.
[51] Mavrogenis G, Hochberger J, Deprez P, et al. Technological review on endoscopic submucosal dissection: available equipment, recent developments and emerging techniques. Scand J Gastroenterol 2017;52:486-498.
[52] Arao M, Ishihara R, Tonai Y, et al. Comparison of ENDO CUT mode and FORCED COAG mode for the formation of stricture after esophageal endoscopic submucosal dissection in an in vivo porcine model. Surg Endosc 2018;32: 2902-2906.
[53] Tonai Y, Ishihara R, Yamasaki Y, et al. Impact of electrosurgical unit mode on post esophageal endoscopic submucosal dissection stricture in an in vivo porcine model. Endosc Int Open 2018;6:E376-E381.
[54] Hirschowitz BI. Photography through the fiber gastroscope. Am J Dig Dis 1963;8:389-395.
[55] Niwa H. The History of Digestive Endoscopy. In: Niwa H, Tajiri H, Nakajima M, Yasuda K, editors. New Challenges in Gastrointestinal Endoscopy. Tokyo. Springer Japan, 2008. p. 3-28.
[56] Kalloo AN, Singh VK, Jagannath SB, et al. Flexible transgastric peritoneoscopy: a novel

approach to diagnostic and therapeutic interventions in the peritoneal cavity. Gastrointest Endosc 2004;60:114-117.

[57] Sumiyama K, Gostout CJ, Rajan E, et al. Transesophageal mediastinoscopy by submucosal endoscopy with mucosal flap safety valve technique. Gastrointest Endosc 2007;65:679-683.

[58] Pasricha PJ, Hawari R, Ahmed I, et al. Submucosal endoscopic esophageal myotomy: a novel experimental approach for the treatment of achalasia. Endoscopy 2007;39: 761-764.

[59] Inoue H, Minami H, Kobayashi Y, et al. Peroral endoscopic myotomy (POEM) for esophageal achalasia. Endoscopy 2010;42:265-271.

[60] Jawaid S, Draganov PV, Yang D. Esophageal POEM: the new standard of care. Transl Gastroenterol Hepatol 2020;5:47.

[61] Vaezi MF, Pandolfino JE, Yadlapati RH, et al. ACG clinical guidelines: diagnosis and management of achalasia. Am J Gastroenterol 2020;115:1393-1411.

[62] Hayat M, Yang D, Draganov PV. Third-space endoscopy: the final frontier. Gastroenterol Rep (Oxf). 2023;11:goac077.

[63] Ishida T, Toyonaga T, Ohara Y, et al. Efficacy of forced coagulation with low high-frequency power setting during endoscopic submucosal dissection. World J Gastroenterol 2017;23:5422-5430.

[64] Bai Y, Yang F, Liu C, et al. Expert consensus on the clinical application of high-frequency electrosurgery in digestive endoscopy (2020, Shanghai). J Dig Dis 2022;23:2-12.

Progress in Medical Devices
eISSN: 2957-5478

Review Article https://doi.org/10.61189/871955jstyqr

Analysis and modeling of forced-damped vibrations and their applications in medicine

Zine Ghemari

Electrical Engineering Department, Mohamed Boudiaf University of M'sila, 28000, Algeria

Corresponding author: Zine Ghemari.

Declaration of conflict of interest: None.

Received December 20, 2023; Accepted February 27, 2024; Published March 31, 2024

Highlights

- The study explores how forced-damped vibrations can be applied in various medical contexts. This may include using vibrations for medical imaging techniques such as ultrasound or MRI, where vibrations are applied to the body to generate images of internal structures.
- Vibrations can also be utilized for tissue characterization, diagnosis of medical conditions, and therapeutic interventions such as vibration therapy for rehabilitation or pain management.

Abstract

Forced-damped vibrations are pivotal in various medical applications, significantly contributing to the examination of tissue mechanical properties, development of medical devices, and understanding of biological systems' complexities. These vibrations represent the dynamic behavior of systems subjected to external forces and damping, where an external force continues to act, and damping determines the rate of energy dissipation. Advanced exploration of damping properties has led to the creation of novel technologies and methods, enhancing our ability to probe and manipulate the complex mechanical dynamics of biological tissues.

Keywords: Analysis, modeling, damped vibrations, medicine

Introduction

Vibrational phenomena are ubiquitous in the medical field, observed in a myriad of contexts [1]. Defined as the repetitive oscillatory motion around a stable point, these phenomena range from the microscopic level to large structural scales [2, 3]. In healthcare, vibrations take various forms, including mechanical vibrations in medical equipment, acoustic vibrations affecting hearing, and electromagnetic vibrations utilized in imaging technologies like MRI [4-6]. Analyzing these vibrations is vital, as they influence the design and functionality of diagnostic instruments, imaging systems, and therapeutic devices [7].

Vibrations in medical devices are characterized by distinct mechanisms, leading to their categorization into free, forced, damped, and resonance vibrations [8-12]. This classification aids in understanding their unique behaviors and effects in medical settings [13]. Free vibrations occur without external force, while forced vibrations arise from external stimuli. Damped vibrations gradually lose energy, and resonance vibrations occur at a specific frequency [14]. This classification is particularly relevant in medical applications, influencing the design and operation of medical equipment, diagnostic procedures, and therapeutic devices [15, 16].

Free vibrations are initiated when a system is set into motion and allowed to oscillate without any external forces [17, 18]. This category of vibration is distinctly defined by the system's natural frequency, a property dictated by its mass and stiffness characteristics. In the realm of medical devices, understanding and analyzing free vibrations is crucial, particularly in the design and operation of medical devices and instruments. Independent oscillations can significantly influence both performance and accuracy [19]. The natural frequency is vital for

Address correspondence to: Zine Ghemari, Electrical Engineering Department, Mohamed Boudiaf University of M'sila, P.O. Box 166, Ichbilya, M'Sila 28000, Algeria. E-mail: ghemari-zine@live.fr.

understanding the intrinsic vibrational behavior of these systems in medical contexts [20].

Forced vibrations occur when an external force or stimulus is applied to a system, causing it to vibrate at a frequency that differs from its natural frequency [21, 22]. This vibration category is marked by its variability, including both periodic and non-periodic patterns [23, 24]. The system's response to forced vibrations is contingent upon the specific attributes of the forcing function and the inherent properties of the system [25-27]. Recognizing the effects of forced vibrations is essential in medical settings, as external forces can alter the behavior of medical devices, diagnostic tools, and therapeutic instruments [28-30]. A deep understanding of these vibrational dynamics is key to optimizing the design and function of medical systems, thereby ensuring better precision and effectiveness [31, 32].

Resonance vibrations occur when an external force or stimulus matches a system's natural frequency, leading to significantly amplified oscillations [33]. This enhancement of vibrations can result in excessive, potentially harmful oscillations [34, 35]. In the medical field, where precision and stability are crucial, uncontrolled resonance vibrations pose significant risks [36, 37]. Thus, effective control and improvements are essential to prevent the detrimental effects of increased vibrations on medical devices, instruments, and structures [38, 39].

Damped vibrations represent a convergence of engineering innovation and healthcare progress [40]. With their controlled and reduced oscillations, damped vibrations serve a critical and diverse role in medicine [41, 42]. From diagnostic instruments to therapeutic strategies, the incorporation of damped vibrations underscores a collaborative, multidisciplinary approach dedicated to enhancing patient care, refining diagnostic capabilities, and propelling the evolution of medical technologies [43-46]. This exploration delves into the varied applications of damped vibrations, highlighting their essential contribution to diagnostic processes, therapeutic approaches, and the overall goal of achieving optimal patient outcomes in the ever-evolving medical landscape [47, 48].

Furthermore, the researches majored in tissue engineering and regenerative medicine leverages controlled vibrations to foster cell growth and direct tissue regeneration processes [49]. The application of damped vibrations in biomechanics research contributes to a deeper understanding of human movement, aiding in the development of rehabilitation strategies and orthopedic interventions [50, 51].

Applications of damped vibration in medicine

Damped vibrations are applied diversely within the medical sector, encompassing areas such as diagnostic imaging, medical devices, tissue engineering, and biomechanics research. The strategic implementation and exploration of damping characteristics play a pivotal role in driving forward medical technology, enhancing diagnostic procedures, and refining therapeutic practices [52].

Medical imaging

In the realm of medical imaging, damped vibrations serve to bolster diagnostic precision. Techniques like elastography utilize damped vibrations to evaluate tissue stiffness, employing induced vibrations to gather data on the mechanical properties of tissues. This approach is invaluable for identifying irregularities or diseases in organs. Specifically, variations in liver stiffness assessed through this method can reveal conditions such as cirrhosis, showcasing the critical role of damped vibrations in diagnosing organ pathologies [52].

Ultrasound Imaging: Damped vibrations are integral to ultrasound imaging, where acoustic waves generate images of internal body structures. A deep understanding of the damping characteristics of tissues enhances the optimization of imaging techniques, leading to improved diagnostic accuracy [53].

MRI: In MRI, an appreciation of damped vibrations is crucial for the development of pulse sequences and optimizing image quality.

Biomechanics and tissue characterization

Damped vibrations are pivotal in biomechanics research, enabling the study of human body movement and its mechanical behaviors. This includes examining the damping properties of joints, bones, and soft tissues. Such researches, which are indispensable for crafting rehabilitation methods, elucidating injury mechanisms, and advancing the design of orthopedic implants [52].

Simulating damped vibrations in a hypothetical system offers a parallel to biomechanical systems or tissues, where variables such as mass, stiffness, and damping ratio are tailored to mirror the specific characteristics of the biomechanical system or tissue in focus (**Figure 1**).

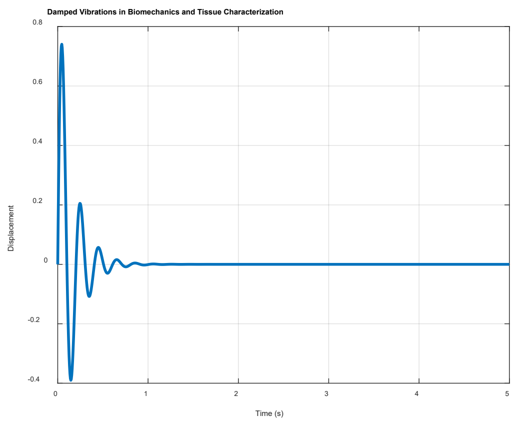

Figure 1. Damped vibration in biomechanics and tissue characterization.

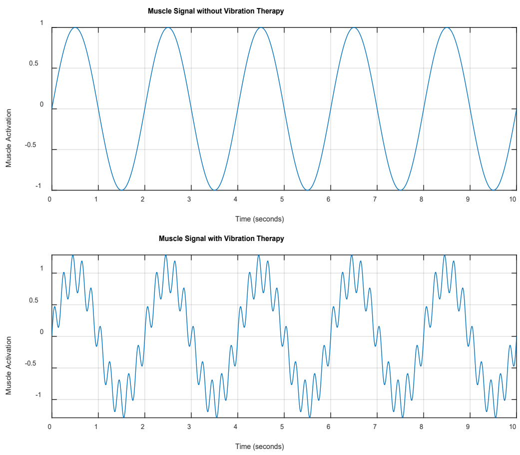

Figure 2. Representation of vibration therapy.

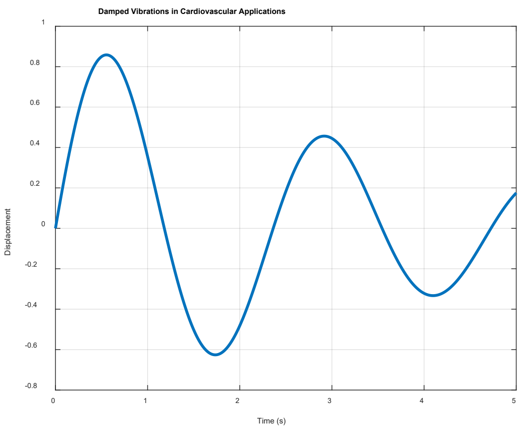

Figure 3. Damped vibration in cardiovascular application.

Figure 1 provides a detailed visualization of biomechanical systems or tissue characterization, underscoring the necessity of employing physiological parameters and a sophisticated model for accuracy. The integration of actual biomechanical data is crucial for augmenting the realism and reliability of our simulations.

Vibration therapy

Within the realm of medical treatments, vibration therapy leverages controlled vibrations for therapeutic benefits. This innovative therapy has been investigated for its potential to address a range of medical issues, particularly musculoskeletal disorders and rehabilitation needs. Although implementing vibration therapy requires a nuanced understanding and is often tailored to specific medical scenarios, a hypothetical MATLAB example offers a simplified model to demonstrate the principles of vibration therapy (**Figure 2**).

Figure 2 is a MATLAB example that simulates muscle signals over time to depict muscle activation both without and with vibration therapy. The lower subfigure introduces a controlled vibration signal, adding a sinusoidal component, to mimic the effects of vibration therapy on muscle activation. In practical scenarios, the selection of vibration parameters and their impact on muscle response are complex, necessitating thorough analysis and experimentation. MATLAB is extensively used by researchers and healthcare practitioners for advanced signal processing and analysis, enabling a comprehensive study of vibration therapy's effects on various physiological parameters [54].

Cardiovascular applications

Developing a detailed MATLAB application for modeling damped vibrations in cardiovascular applications entails intricate modeling and simulations, which extend beyond the topic of this review. The simulation of damped vibrations in a hypothetical system can serve as a model for cardiovascular dynamics, with adjustments to parameters like mass, stiffness, and damping ratio to reflect the specific characteristics of the cardiovascular system under study.

For a more precise modeling of cardiovascular dynamics, employing physiological parameters and a sophisticated model is essential (**Figure 3**). Furthermore, the inclusion of actual cardiovascular data would significantly improve the realism and accuracy of our simulations.

Figure 3 illustrates the specific behaviors of damped vibrations within a cardiovascular context, potentially showcasing the oscillatory movements within cardiovascular devices or systems. Such visualizations are crucial for understanding the dynamic aspects of cardiovascular mechanics.

Blood Flow Analysis: Damped vibrations are instrumental in analyzing blood flow dynamics, particularly in examining arterial elasticity and in the design and optimization of cardiovascu-

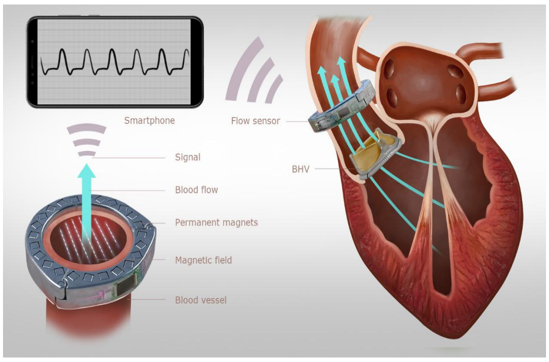

Figure 4. Prosthetic heart valves monitoring. The reference was cited from [56].

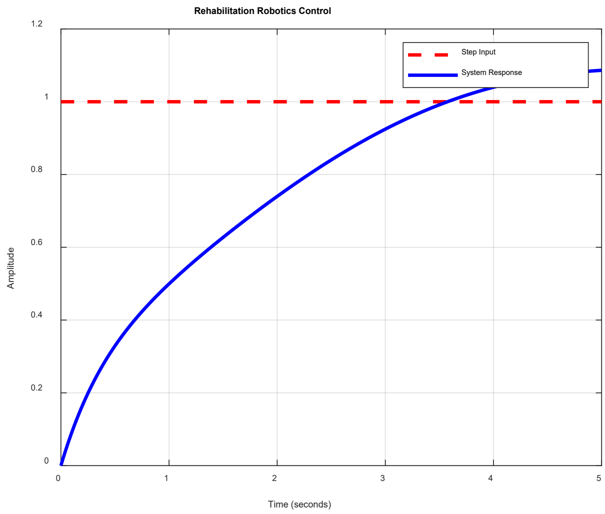

Figure 5. Results of a simple second-order plant model and a PID controller in a rehabilitation robotics.

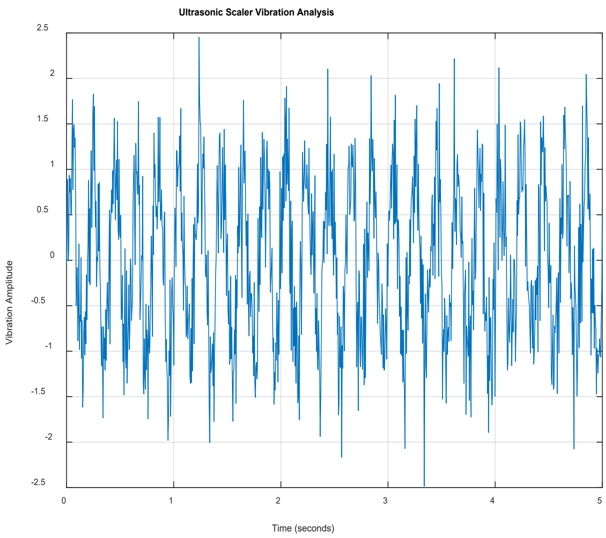

Figure 6. Vibration amplitude of ultrasonic scaler vibration analysis.

lar devices.

Heart Valve Dynamics: Analyzing the damped vibrations in heart valves aids in understanding their function and contributes to the development of artificial heart valves (see **Figure 4**).

Rehabilitation robotics

Rehabilitation robotics is tailored to meet a wide array of user needs, with damped vibrations playing a key role in enabling user-specific customization. This allows for adjustments to be made according to individual preferences, comfort levels, and specific rehabilitation goals, thereby enhancing both the user experience and the effectiveness of the rehabilitation process.

Incorporating advanced sensor technologies into robotic exoskeletons and assistive devices, and coupling these with damped vibrations, facilitate precise control and coordination. This integration ensures that devices can intelligently adapt to the user's movements and intentions. The strategic application of damped vibrations within rehabilitation robotics significantly boosts the success of rehabilitation programs. By offering a controlled and comfortable setting for movement, individuals in rehabilitation are able to participate more fully in therapeutic exercises, leading to improved recovery outcomes [54].

Ensuring a comfortable and safe experience is crucial for the acceptance and compliance with rehabilitation robotics. Damped vibrations are instrumental in fostering a positive interaction between the user and the robotic device, enhancing user engagement in rehabilitation activities and potentially accelerating recovery [55].

Rehabilitation robotics frequently employs MATLAB for control system design, data analysis, and simulation tasks. **Figure 5** illustrates the results of such simulations.

Figure 5 serves as a graphical representation that showcases the outcomes and performance of a control system in rehabilitation robotics, featuring a straightforward second-order plant model paired with a PID controller. The details depicted within the figure provide valuable insights into the control system's dynamic behavior and its effectiveness within a rehabilitative setting.

Dental applications

Tooth vibration analysis employs specialized instruments designed to initiate controlled vibrations and accurately measure the ensuing responses. These measurements yield crucial data regarding the dynamic behavior of teeth under various dental interventions.

For instance, during tooth drilling procedures, the interaction between dental instruments

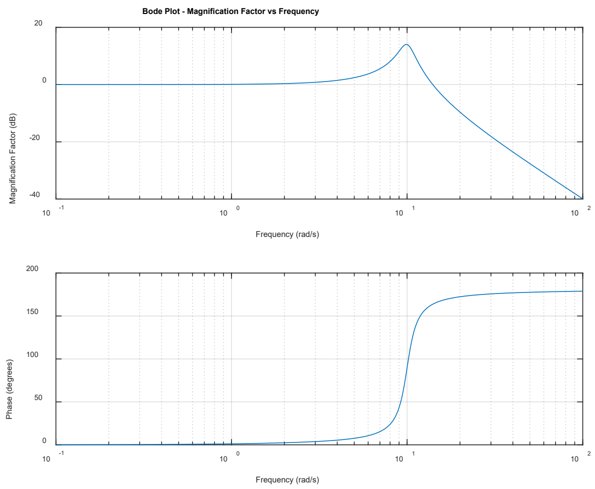

Figure 7. Bode diagram of the magnification factor.

and the tooth structure gives rise to vibrations. Through damped vibration analysis, dentists gain a refined understanding of the mechanical responses of teeth to differing procedures, enhancing both diagnostic capabilities and treatment precision [55].

The process of analyzing vibration amplitudes from an ultrasonic scaler with MATLAB typically involves the manipulation and graphical representation of data derived from the scaler's vibrations. **Figure 6** illustrates the simulation outcomes for the ultrasonic scaler application [55].

Figure 6 delves into the analysis of vibration amplitude in an ultrasonic scaler, offering critical insights that are essential for the optimization of the scaler's design, performance, and safety in dental or medical contexts.

The analysis of tooth vibrations aids in the assessment of structural integrity. Variations in vibration patterns can signal the presence of dental conditions such as cavities, cracks, or structural abnormalities. Such detailed information is invaluable to dentists for accurate diagnosis and the formulation of effective treatment plans [55].

Continued advancements in tooth vibration analysis are driving the development of new dental technologies and methodologies. This research-centric approach is pivotal in refining dental procedures, elevating diagnostic precision, and progressing the field of dental care.

Moreover, integrating tooth vibration analysis into dental education is crucial for the comprehensive training of future dental professionals. It equips aspiring dentists with a deep understanding of the mechanical dynamics involved in dental procedures, promoting a more knowledgeable and proficient approach to patient care [55].

Magnification factor

The magnification factor, also known as the amplification factor or gain, is crucial in understanding how a dynamic system amplifies or attenuates input vibrations at specific frequencies. It is typically depicted as a function of frequency, illustrating the system's behavior over a spectrum of frequencies [56].

In the context of a linear, single-degree-of-freedom system subjected to forced-damped vibrations, the magnification factor (M) is commonly defined as the ratio of the response amplitude (X) to the amplitude of the applied force (F_0). This relationship is mathematically represented as [38]:

$$M(\omega) = X/F_0 \qquad (1)$$

This formula of magnification factor is expressed as:

$$M(\omega) = 1/[(1 - (\omega/\omega_n)^2)^2 + (2\zeta\omega/\omega_n)^2]^{1/2} \qquad (2)$$

Where:
ω is the frequency of the input vibration.
ωn is the natural frequency of the system.
ζ is the damping ratio

The magnification factor is affected by the natural frequency and damping ratio of the system. When plotted against frequency, the Bode plot allows engineers and researchers to analyze how the system responds to different input frequencies. A peak in the magnification factor indicates resonance, where the system's response is magnified (see **Figure 7**).

The Bode diagram showcasing the magnification factor as a function of frequency offers a comprehensive representation of a dynamic system's response characteristics. This graphical representation is invaluable in analyzing structural, mechanical systems, and vibrational behaviors, providing critical insights into how these systems respond to varying frequencies.

Conclusion

Damping is paramount in the realm of forced-damped vibrations, serving to dissipate energy and diminish the amplitude of oscillations over time. The presence of various damping forms, such as friction or fluid resistance, influences a system's response, guiding it towards equilibrium. Forced-damped vibrations are described through mathematical models, typically differential equations, facilitating a deep understanding of the system's dynamics. This includes insights into steady-state and transient responses, resonance frequencies, and additional pivotal properties.

The exploration of forced-damped vibrations enables engineers to design resilient structures, enhance machine efficiency, and ensure the stability and safety of mechanical systems. Furthermore, the application of damped vibrations in medicine emerges as a critical and multifaceted component of healthcare and biomedical research. Through the investigation of damped vibrations, significant advancements have been made, particularly in understanding the mechanical properties of biological tissues. This knowledge is instrumental across a wide range of medical applications, underscoring the indispensable role of damped vibrations in advancing healthcare.

References

[1] Liu Z, He Q, Chen S, et al. Time-Varying Motion Filtering for Vision-Based Nonstationary Vibration Measurement. IEEE Trans Instrum Meas 2020;69:3907-3916.

[2] Ma Z, Luo Y, Xie S, et al. Active Vibration Control of Cantilever Beam in fast Maneuvering Flight Environment. 2022 16th Symposium on Piezoelectricity, Acoustic Waves, and Device Applications (SPAWDA) 2022;351-355.

[3] Li C, Li J, Fang XL, et al. Application of a Method of Identifiying Instantaneous Shaft Speed from Spectrum in Aeroengine Vibration Analysis. 2022 Global Reliability and Prognostics and Health Management (PHM-Yantai) 2022;1-7.

[4] Zhao M, Shen X, Jiang F. Research on Mechanical Vibration Measurement Method Based on Event Camera. 2023 3rd International Conference on Energy Engineering and Power Systems (EEPS) 2023;528-532.

[5] Li S, Xiong Y, Ren Z, et al. Ultra-micro Vibration Measurement Method Using CW Doppler Radar. 2020 International Conference on Sensing, Measurement & Data Analytics in the era of Artificial Intelligence (ICSMD) 2020;235-237.

[6] Li S, Xiong Y, Zhou P, et al. mmPhone: Sound Recovery Using Millimeter-Wave Radios With Adaptive Fusion Enhanced Vibration Sensing. IEEE Trans Microw Theory Tech 2022;70:4045-4055.

[7] Reguieg SK, Ghemari Z, Benslimane T. Extraction of the relative sensitivity model and improvement of the piezoelectric accelerometer performances. 2018 International Conference on Signal, Image, Vision and their Applications (SIVA) 2018;1-5.

[8] Ghemari Z, Salah S, Defdaf M. Appropriate Choice of Damping Rate and Frequency Margin for Improvement of the Piezoelectric Sensor Measurement Accuracy. J Adv Manuf Syst 2021;20:537-548.

[9] Zou XY, Jiang GH, Ye LC, et al. Surface vibration and noise analysis of POD Propeller of Construction Scientific Research Ship. 2021 6th International Conference on Power and Renewable Energy (ICPRE) 2021;1519-1523.

[10] Berta Š, Goga V, Murín J. Active Vibration Damping of Cantilever Beam using LabVIEW. 2022 Cybernetics & Informatics (K&I) 2022;1-6.

[11] Xiong Y, Liu Z, Li S, et al. Scanning Microwave Vibrometer: Full-Field Vibration Measurement via Microwave Sensing With Phase-Encoded Beam Scanning. IEEE Trans Instrum Meas 2023;72:1-11.

[12] Cao H, Huang T, Lu L, et al. Research on Quasi-zero Stiffness Vibration Isolation Technology of Distribution Transformer. 2021 IEEE 4th International Conference on Automation, Electronics and Electrical Engineering (AUTEEE) 2021;613-617.

[13] Ghemari Z, Saad S. Parameters improvement and suggestion of new design of capacitive accelerometer. Analog Integr Circuits Signal Process 2017;92:443-451.

[14] Ghemari Z, Saad S, Amrouche A, et al. New model of piezoelectric accelerometer relative movement modulus. Trans Inst Meas Control 2014;37:932-941.

[15] Ghemari Z, Saad S. Modeling and enhancement of mechanical sensitivity of vibration sensor. J Vib Control 2013;20:2234-2240.

[16] Ghemari Z, Chouaf F, Saad S. New Formula for the Piezoresistive Accelerometer Motion Acceleration and Experimental Validation. J Adv Manuf Syst 2017;16:57-65.

[17] Ghemari Z, Lakehal A, Saad S. Minimisation of resonance phenomena effect of piezoresistive accelerometer. 2015 4th International Conference on Systems and Control (ICSC) 2015;243-246.

[18] Ghemari Z, Saad S. Improvement of piezoresistive accelerometer performance. 3rd International Conference on Systems and Control 2013;759-762.

[19] Wang D. Analysis and Solution of Abnormal Vibration of Elevator Box Based on Information Technology. 2022 International Conference on Artificial Intelligence in Everything (AIE) 2022;306-309.

[20] Zhu M, Feng Y, Zhang Y, et al. A Noval Building Vibration Measurement system based on

Computer Vision Algorithms. 2022 IEEE 17th Conference on Industrial Electronics and Applications (ICIEA) 2022;1146-1150.
[21] Lin F, Zheng H, Xiang B, et al. Vibration-Induced Noise in Extremely Low-Frequency Magnetic Receiving Antennas. IEEE Antennas Wirel Propag Lett 2021;20:913-917.
[22] Long G, Zheng K, Liu Y, et al. Experimental Study on Vibration Mechanism and Prevention Technology of Heavy Load Switchgear. 2022 IEEE International Conference on High Voltage Engineering and Applications (ICHVE) 2022;1-4.
[23] Ghemari Z. Upgrading of piezoresistive accelerometer response. 2016 8th International Conference on Modelling, Identification and Control (ICMIC) 2016;544-547.
[24] Ghemari Z, Saad S. Reducing the Measurement Error to Optimize the Sensitivity of the Vibration Sensor. IEEE Sens J 2014;14:1527-1532.
[25] Ghemari Z, Saad S. Defects Diagnosis by Vibration Analysis and Improvement of Vibration Sensor Measurement Accuracy. Sens Lett 2019;17:608-613.
[26] Mishra M, Srivastav CK, Kumar S. Free vibration analysis using dynamic stiffness method and first-order shear deformation theory for a functionally graded material plate. Mater Today: Proc 2024;98:7-15.
[27] Khan NU, Ahmad S, Janjua MM, et al. The Design of Vibration Nomograph for the Vehicle Vibrations Affecting Man. 2022 Advances in Science and Engineering Technology International Conferences (ASET) 2022;1-7.
[28] Noubissi RK, Daosheng L, Boxue D. Study on Harmonic Response Analysis and Vibration Reduction of Amorphous Metal Alloy Transformer. 2023 IEEE 4th International Conference on Electrical Materials and Power Equipment (ICEMPE) 2023;1-4.
[29] Pan K, Zhang W. Dynamic modeling and vibration reduction analysis of a negative Poisson's ratio honeycomb foundation support. 2020 5th International Conference on Mechanical, Control and Computer Engineering (ICMCCE) 2020;524-527.
[30] Ghemari Z et al. Mechanical resonator sensor characteristics development for precise vibratory analysis. Sens Imaging 2021, 22:40
[31] Ghemari Z, Belkhiri S, Saad S. Improvement of the Relative Sensitivity for Obtaining a High Performance Piezoelectric Sensor. IEEE Instrum Meas Mag 2023;26:49-56.
[32] Ghemari Z, Belkhiri S, Saad S. Appropriate choice of Capacitive sensor bandwidth (Preprint). Res Sq 2023.
[33] Okada T, Isobe M, Kosaka T, et al. Study on Electric Motor Vibration Suppression by Active Dynamic Vibration Absorber. 2023 IEEE International Electric Machines & Drives Conference (IEMDC) 2023;1-7.
[34] Xu C, Yin Z, Li X, et al. Remote control of eddy current damping vibration experiment system. 2021 International Conference on Cyber-Physical Social Intelligence (ICCSI) 2021;1-5.
[35] Yan H, Zhang C, Wang G. Experimental Study on Dual-channel Active Control Method for Transverse Vibration of Ship Propulsion Shaft System. 2023 7th International Conference on Transportation Information and Safety (ICTIS) 2023;1353-1356.
[36] Ghemari Z, Belkhiri S. Capacitive Sensor Accuracy Optimisation by the Frequency Range Appropriate Choice (Preprint). Res Sq 2021.
[37] Ghemari Z. Enhancement of the vibratory analysis technique by the accelerometer characteristics evolution. The 7th International Conference on Control Engineering & Information Technology 2019.
[38] Ghemari Z, Belkhiri S, Saad S. A piezoelectric sensor with high accuracy and reduced measurement error. J Comput Electron 2024.
[39] Neamtu A, Simoiu D, Ursu AR, et al. Analysis of the Relaxation Effect by Vibrations on Some Rheological Models of Tissues. 2022 IEEE 16th International Symposium on Applied Computational Intelligence and Informatics (SACI) 2022;000204-000206.
[40] Hao C, Xinyu D, Ling L, et al. Test and Analysis of Acoustic and Vibration Characteristics of Transformer in Winding and Iron Core Loose. 2023 IEEE 3rd International Conference on Power, Electronics and Computer Applications (ICPECA) 2023;1644-1647.
[41] Mistry C, Ghosh SK. Effect of Vibration on the Cathode Lead of Electron Gun Assembly of the Travelling Wave Tube. 2020 URSI Regional Conference on Radio Science (URSI-RCRS) 2020;1-2.
[42] Zheng L, Chen W, Huo D, et al. Design, Analysis, and Control of a Two-Dimensional Vibration Device for Vibration-Assisted Micromilling. IEEE ASME Trans Mechatron 2020;25:1510-1518.
[43] Song H, Song E, Liu Y, et al. Miniature FBG Vibration Sensor With High Performance and Low Angle Dependence for Two-Dimensional Vibration Measurement. IEEE Trans Instrum Meas 2023;72:1-11.
[44] Wang B, Zhang H, Cao M, et al. Parameter analysis and experimental verification of dynamic vibration absorption design for transformer tank wall. 2022 7th Asia Conference on Power and Electrical Engineering (ACPEE) 2022;830-837.
[45] Li H, Deng Z, Zhao J, et al. Influence of Electromagnetic Shunt Damper on Nonlinear Vibration of HTS Maglev System. IEEE Trans Appl Supercond 2021;31:1-4.

[46] Ding Y, Zhong Y, Wang X, et al. Difference and Analysis of Mechanical Vibration Signal Characteristics between Mechanical Defects and Partial Discharge Defects of Gas Insulated Switchgear. 2021 IEEE 5th International Conference on Condition Assessment Techniques in Electrical Systems (CATCON) 2021;211-214.

[47] Xiao Y, Cao Ja, Xiong X, et al. Research on Vibration Measurement Method and Analysis of Air-core Reactor. 2020 IEEE International Conference on High Voltage Engineering and Application (ICHVE) 2020;1-4.

[48] Wang Y, Xia Z, Xie R. Vibration control technology of ship transmission based on machine learning. 2022 International Conference on Artificial Intelligence in Everything (AIE) 2022;580-584.

[49] Zhang YS, Li YS, Liu SH. Vibration analysis of IEC 61373 standard based on measured data. 2021 7th International Symposium on Mechatronics and Industrial Informatics (ISMII) 2021;20-23.

[50] Wang Q, Lei X. The Method for Identifying Rotating Blade Asynchronous Vibration and Experimental Verification. 2020 11th International Conference on Prognostics and System Health Management (PHM-2020 Jinan) 2020;564-568.

[51] Liu Q, Fu CJ, Wang YL, et al. Simulation Analysis of Transmission Wire Breeze Vibration. 2022 6th International Conference on Power and Energy Engineering (ICPEE) 2022;163-168.

[52] Tabatabai H, Oliver DE, Rohrbaugh JW, et al. Novel Applications of Laser Doppler Vibration Measurements to Medical Imaging. Sens Imaging 2013;14:13-28.

[53] Nastar C, Ayache N. Frequency-based nonrigid motion analysis: application to four dimensional medical images. IEEE Trans Pattern Anal Mach Intell 1996;18:1067-1079.

[54] Saggini R. The Mechanical Vibration: Therapeutic Effects and Applications. The United Arab Emirates. Bentham Science Publishers, 2017.

[55] Issurin VB. Vibrations and their applications in sport. A review. J Sports Med Phys Fitness 2005;45:324-336.

[56] Vennemann B, Obrist D, Rösgen T. A smartphone-enabled wireless and batteryless implantable blood flow sensor for remote monitoring of prosthetic heart valve function. PLoS One 2020;15:e0227372.

Progress in Medical Devices
eISSN: 2957-5478

Review Article https://doi.org/10.61189/390527zficik

Research progress of biodegradable staples in gastrointestinal anastomosis

Xue Cai, Lin Mao, Junjie Shen, Yujie Zhou, Chengli Song

Shanghai Institute for Minimally Invasive Therapy, School of Health Science and Engineering, University of Shanghai for Science and Technology, Shanghai 20093, China

Corresponding author: Lin Mao.

Declaration of conflict of interest: None.

Received February 15, 2024; Accepted February 28, 2024; Published March 31, 2024

Highlights

- Biodegradable staples have the high biodegradability, good mechanical, and biocompatibility properties.
- The mechanical properties of biodegradable staples can be adjusted by structure optimizations.
- Biodegradable will be widely used in gastrointestinal anastomosis.

Abstract

Since the 1960s, anastomosis instruments have become integral in gastrointestinal procedures, employing Titanium (Ti) alloy staples. These staples, however, remain permanently in the body, potentially inciting inflammatory reactions, compromising computed tomography scans, and causing diagnostic inaccuracies. This scenario underscores the imperative for biodegradable surgical staples, spurring research into materials that exhibit both superior biodegradability and mechanical integrity. Current investigations are focused on Magnesium (Mg), Zinc (Zn), and their alloys for their exemplary biodegradability, mechanical strength, and biocompatibility, making them promising candidates for gastrointestinal anastomosis. This review encapsulates the latest advancements in biodegradable surgical staples, emphasizing material and structural enhancements. It details the mechanical attributes of wires intended for staple fabrication, the corrosion dynamics across varied environments such as in vitro immersion solutions and in vivo implantation sites and the impact of structural refinements on staple biodegradability. Additionally, it contrasts the benefits and limitations of Mg-based and Zn-based staples and offers insights into the potential and hurdles in developing biodegradable surgical staples, thereby fostering further exploration in this field.

Keywords: Surgical staple, gastrointestinal anastomosis, biodegradable material, structural optimization, finite element analysis

Introduction

In clinical settings, surgical staples, predominantly crafted from Titanium (Ti) alloy, have revolutionized the healing and reconstruction processes in gastrointestinal anastomosis, spanning the gastrointestinal tract to the small intestine [1-3]. Staples offer advantages over traditional suturing by reducing operative durations, minimizing postoperative complications, and alleviating patient discomfort [4]. Nevertheless, the permanent presence of Ti alloy staples within the body can provoke inflammatory responses and other severe complications [5]. Thus, there is a pressing need for the development of biodegradable staples, which promise to eliminate long-term adverse effects associated with their non-degradable counterparts [6]. Since 2016, biodegradable staples have garnered significant attention for their potential in facilitating the healing and reconstruction of the stomach and intestinal tract [7].

In traditional gastrointestinal anastomosis, the paramount considerations for surgical staples are adequate mechanical strength, optimal blood supply, and the absence of tension, all of which are crucial for effective wound healing [8]. The diverse implantation environments within gastrointestinal anastomosis, including varying

Address correspondence to: Lin Mao, Shanghai Institute for Minimally Invasive Therapy, School of Health Science and Engineering, NO.516, Jungong Road, Shanghai 200093, China. Email: linmao@usst.edu.cn.

Table 1. Recent studies on biodegradable surgical staples in gastrointestinal anastomosis

Materials	The yield tensile strength	The ultimate tensile strength	Elongation	Soak solution	Corrosion behavior	Experimental animal type	The implan-tation cycle	Refer-ence
HP Mg (Ø 0.26 mm, 2016)	147 ± 8 MPa	196 ± 5 MPa	14.6 ± 5%	The m-SBF	The staples were not absorbable completely for 9 weeks and the remained part kept homogeneous shape without fracture.	Pigs (stomach)	9 weeks	[7]
HP Mg (Ø 0.26 mm, 2017)	147 ± 8 MPa	196 ± 5 MPa	14.6 ± 5%	The intestinal juice/Hanks' solution	0.49 mm/year (intestinal juice) / 0.34mm/year (Hanks' solution)	Adult minipigs (small intestine)	1 month	[10]
HP Mg (Ø 0.26 mm, 2017)	147 ± 8 MPa	196 ± 5 MPa	14.6 ± 5%			Mice (rectal)	7 days	[11]
HP Mg (Ø 0.26 mm, 2021)	147 ± 8 MPa	196 ± 5 MPa	14.6 ± 5%	The m-SBF	The degradation rate of 3.1 mm/year on the 3rd day and then the corrosion rate gradually tended to be about 1 mm/year.	New Zealand rabbits (small intestine)	7 weeks	[12]
Mg-6Zn (Ø 1 mm, 2013)	169.5 ± 3.6 MPa	279.5 ± 2.3 MPa	18.8 ± 0.8%	The intestinal juice	0.16 mm/year(in vitro) / 2.32 mm/year(in vivo)	Sprague–Dawley rats (cecum)	4 weeks	[13]
Mg-5Zn (Ø 0.23mm, 2023)				The HBSS/ SCF	The staples in SCF degraded at a faster rate in the first 3 days, approximately three times higher than those in Hanks' solution.			[14]
ZN20 (Ø 0.23mm, 2021)		256 ± 8 MPa	12.56% ± 0.66%	Drainage fluid from the abdomen andsplenic fossa, the gastric tube, and the duo-denum	The staples in vitro corroded completely within 6 days / The staples in vivo corroded completely within about 8 weeks.	Female New Zealand rabbits (stomach and intestine)	1, 2, 4 and 8weeks	[16]
FA sorb Mg™ (Ø 0.25mm, 2019)	260 ± 0 MPa	290 ±1 MPa	22 ± 1%	The artificial intestinal juice	The products of corrosion covered all staples after four days of immersion	Female adult pigs (small intestine)	4 weeks	[18]
AZ31 (Ø 0.3mm, 2023)		302 ± 4MPa	23 ± 3%	The SCF	The staples remained in its integrated structure after 7 days and completed degradation after 90 days.	Beagle dogs (colon)	7 days (6 dogs) and 90 days (18 dogs)	[4]
Zn alloy 1) / Zn alloy 2) / Zn alloy 3 (Ø 0.4mm, 2020)		212/198/ 200 MPa	19/7/21%	The FeSSIF and HBSS	The corrosion rates of Zn alloy staples 1, 2, and 3 were 0.02 mm/year in HBSS and 0.12, 0.11, and 0.13 mm/year in FeSSIF.	Male New Zealand white rabbits (stomach)	1, 4, 12 weeks	[19]
Zn-0.8 wt.% Li-0.1 wt.% Mn (Ø 0.3 mm, 2020)	390.12 ± 12.45 MPa	530.16 ± 1.62 MPa	68.89 ± 2.68%	The Hanks' solution and SGF	0.843 ± 0.003 mm/year (SGF) / 0.191 ± 0.009 mm/year (Hanks' solution)	Mini fragrant pigs (stomach and intestine)	3 days, 8 weeks, and 12 weeks	[5]

Note: HP Mg, high-purity Magnesium; m-SBF, modified simulated body fluid; Zn, Zinc; Ti, Titanium; HBSS, hank's balanced salt solution; SCF, simulated colon fluid; ZN20, Mg-2Zn-0.5Nd; FA sorb Mg™, Mg-2.5Nd-1Y; Zn alloy 1, Zn-1.0Cu-0.2Mn-0.1Ti; Zn alloy 2, Zn-1.0Mn-0.1Ti; Zn alloy 3, Zn-1.0Cu-0.1Ti; FeSSIF, fed-state simulated intestinal fluid; SGF, simulated gastric fluid.

Table 2. Main characteristics of staples used in gastrointestinal anastomosis

Materials	Advantages	Disadvantages
Ti-based alloys	High biocompatibility and corrosion resistance, fatigue strength, light weight.	Lack of biodegradability.
HP Mg / Mg-based alloys	Biodegradable, excellent biocompatible, broad range of mechanical strength, pro-wound healing degradation products.	Fast corrosion rate, hydrogen gas evolution during biodegradation, prone to stress corrosion cracking.
Zn-based alloys	Biodegradable, good biocompatible, moderate corrosion resistance	Prone to age hardening and creep.

Note: This table was cited from [9, 21]. Ti, Titanium; HP Mg, high-purity Magnesium; Zn, Zinc.

tissues such as the stomach, small intestine, and rectum, present significant challenges in the development of biodegradable staples for these procedures [9]. Unlike conventional staples, biodegradable surgical staples not only must provide robust support throughout the entire healing process without failure but also must degrade safely at a controlled rate within the complex environment of human body, gradually relinquishing their load-bearing capacity as tissues recover [3]. Hence, the researches in terms of biodegradable surgical staples include corrosion and the biocompatibility of Magnesium (Mg) / Zinc (Zn)-based alloy staples in vitro and in vivo, and their mechanical properties.

This review delineates advancements in biodegradable surgical staple technology, focusing on mechanical attributes, corrosion rates across different in vitro and in vivo environments, and the impact of structural enhancements on the performance of these staples, as detailed in **Table 1**. Specifically, it explores the leading Mg-based and Zn-based materials for gastrointestinal anastomosis applications, discussing the deployment strategies of these materials in various implantation sites through both in vitro and in vivo studies. Ultimately, it underscores the challenges associated with employing Mg/Zn-based surgical staples in clinical settings.

Biodegradable surgical staples composed of Mg and its alloys

High-purity (HP) Mg anastomotic staples

In the evolution of biodegradable surgical staples, HP Mg staples have been subject to extensive examination. The inaugural HP Mg staples, designed for gastric anastomosis, were introduced in 2016 [7]. To circumvent stress corrosion after being closed, these staples were engineered with an interior angle of 100°, altering the distribution of residual stress. After nine-week post-implantation in pigs, the HP Mg staples showed robust support and excellent biocompatibility for stomach anastomosis. Subsequently, Qu et al. documented the application of HP Mg staples in small intestine anastomosis of minipigs, demonstrating their ability to provide ample support over one month [10]. Furthermore, the integration of Mg staples into tissue occurred without complications, and the in vivo degradation rate of these bridging surgical staples was determined to be 0.007 mm per month.

More in-depth researches were carried since the discover of that HP Mg staples could influence wound healing processes. In 2017, Xia et al. reported that HP Mg staples could mitigate inflammatory responses in rectal anastomoses by modulating the activities of signaling growth factors [11]. More recently, in 2021, Zan et al. employed HP Mg staples in intestinal closure studies, uncovering their antitumor effects [12]. The release of Mg ions and hydrogen from HP Mg staples, both in vitro and in vivo, was found to inhibit the recurrence of residual tumor cells. These researches attest to the excellent biodegradability of HP Mg anastomotic staples, and their wound healing potential, paving the way for further detailed investigations.

Although HP Mg staples have demonstrated adequate support, favorable biocompatibility, and effective wound healing capabilities in various studies, skepticism remains regarding their clinical application. Concerns particularly revolve around the corrosion rate, hydrogen gas evolution, and stress corrosion during the degradation process, as outlined in **Table 2**. This table was cited from [9, 21]. Consequently, the future research will delve into the safety of HP Mg staples for human use in gastrointestinal anastomosis.

Biodegradable surgical staple composed of Mg alloys

The exploration of gastrointestinal anastomosis utilizing Mg-Zn alloys initially diverged into various methodologies. In 2013, Yan et al.

pioneered the study of Mg-6Zn stapler pins by evaluating their impact on rat cecum incisions, marking the first investigation into the application of Mg-Zn alloys for stapler pins in intestinal reconstruction [13]. Following this, Cheng et al. examined the degradation behavior and practicality of Mg-5Zn staples, finding that these staples degraded uniformly in simulated colon fluid and maintained their effectiveness up to ten days [14]. In 2021, Song et al. explored the potential of Mg-2Zn-0.5Nd (ZN20) alloy as a material for surgical nails [15]. They employed ZN20 alloy wires and surgical sutures to secure the lower margin of the stomach in New Zealand rabbits. At same year, Gao et al. documented the successful deformation of staples made from ZN20 alloy from a U-shape to a B-shape, demonstrating that ZN20 staples possessed adequate mechanical support for anastomosis with a bursting pressure of 40 kPa [16]. In a subsequent study in 2022, Zhang et al. reported that Mg-6Zn-1Mn staples not only showcased high strength (340 MPa) but also displayed satisfactory ductility (10%) [17]. Significantly, the mechanical integrity of the staples was enhanced to 90 hours post-processing by incorporating protein, with all rabbits making a full recovery and resuming normal oral intake.

Beyond the Mg-Zn alloy staples, several other Mg-based staples with superior mechanical properties have been explored for gastrointestinal anastomosis applications. In 2019, Amano et al. highlighted the enhanced mechanical properties of Mg-2.5Nd-1Y (FA sorb Mg™) staples, which demonstrated a yield tensile strength of 260 MPa, an ultimate tensile strength of 290 MPa, and an elongation at break of 22% [18]. The study revealed that FA sorb Mg™ staples could provide robust support for the healing of small intestines. In a 2022 study, Zhang et al. introduced an AZ31 staple designed for colonic anastomosis [4]. Notably, they achieved a moderate degradation rate aligned with the tissue healing timeline for colonic anastomosis through micro-arc oxidation treatment and further enhanced by coating the AZ31 alloy staples with poly-L-lactic acid. The colon wounds exhibited complete recovery after 90 days post-operation, with no instances of leakage or stenosis. Additionally, all 12 dogs in the study fully recovered without any trace of element accumulation in their organs, and no severe inflammation, tissue necrosis, or abnormal hyperplasia was observed during implantation.

While these Mg alloy staples provide adequate support, exhibit desirable biodegradation, and maintain good biocompatibility, the incorporation of other elements into surgical staples for use in human gastrointestinal anastomosis necessitates further investigation. Consequently, a prolonged period of study is essential for Mg alloy staples intended for gastrointestinal anastomosis applications.

Biodegradable surgical staples composed of Zn Alloy

Research on Zn-based alloys for surgical staples is a relatively recent development, with the inaugural study by Amano et al. in 2020 marking a significant milestone. This study explored three Zn alloys (Zn-1.0Cu-0.2Mn-0.1Ti, Zn-1.0Mn-0.1Ti, and Zn-1.0Cu-0.1Ti) as potential materials for gastric resection staples [19]. The Zn alloy staples demonstrated adequate support for gastro-restriction applications during in vivo implantation. Moreover, this study noted tissue inflammatory responses post-implantation, indicating the short-term safety of these Zn-based staples in animal models. Subsequently, Guo et al. introduced a gastrointestinal staple composed of a Zn-0.8Li-0.1Mn alloy, showcasing impressive mechanical properties, including yield tensile strength, ultimate tensile strength, and elongation at 390 MPa, 530 MPa, and 69%, respectively [5]. These Zn-Li-Mn staples exhibited a slower corrosion rate (0.191 ± 0.009 mm/year in Hanks' solution) compared to HP Mg staples (0.34 mm/year), with 89% of the staple remaining after 12 weeks of implantation. The advantages of Zn-based staples lie in their degradation mechanisms: no gas generation, formation of a compact degradation product, good biocompatibility, moderate corrosion resistance, and superior mechanical properties.

Although Mg screws and stents have been utilized clinically, Mg-based staples have yet to advance to clinical trials, with knowledge confined to in vivo studies [8, 20]. The rapid corrosion rate, hydrogen gas evolution, and susceptibility to stress corrosion cracking limit the application of Mg-based staples. In contrast, the slower corrosion rate of Zn alloys allows for a more extended retention of mechanical integrity in staples, despite their susceptibility to age hardening and creep [21]. Nonetheless, current researches on Zn-based staples in gastrointestinal anastomosis have their limitations, indicating a need for more detailed studies.

Structural optimizations of biodegradable surgical staples

To enhance the efficacy of biodegradable surgical staples in clinic, structural optimization

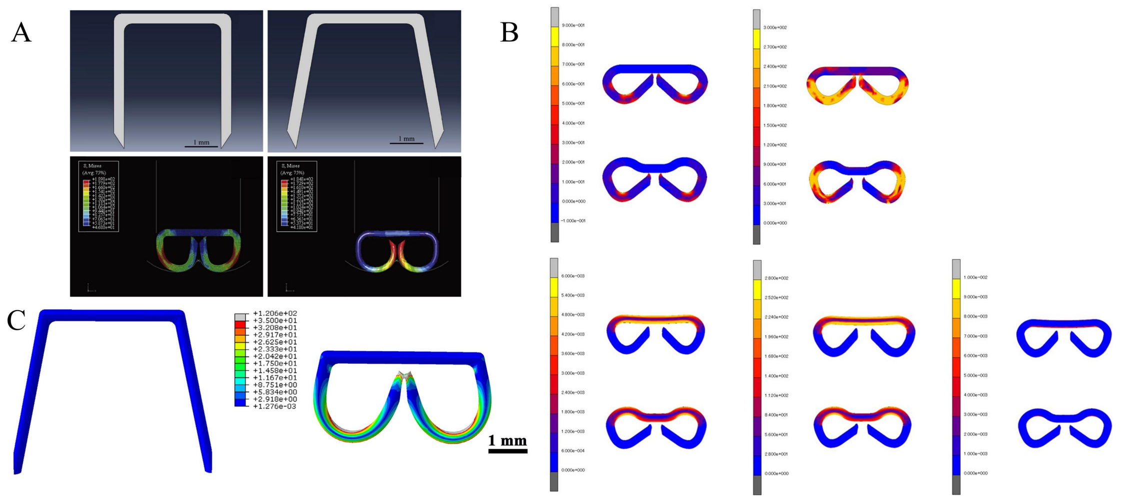

Figure 1. Structural optimizations of biodegradable surgical staples. (A) Structural design and finite analysis on the high-purity Magnesium staple; (B) The Mg-2.5Nd-1Y staple; (C) The Zn-0.8Li-0.1Mn staple. This figure was cited from [5, 7, 18]. Mg, Magnesium; Zn, Zinc.

has emerged as a pivotal strategy for improving the integrity of biodegradable anastomoses. In 2016, Wu et al. undertook a study to refine the design of HP Mg staples for gastric anastomosis through Finite Element Analysis [7]. Their designed the shape of staples in a U-form with interior angles of 90° and 100°, as depicted in **Figure 1A** [7]. The Finite Element Analysis identified the staple with a 100° interior angle as optimal, effectively distributing residual stress at the staple's tip upon closure to mitigate stress corrosion risk. Gao et al. further elucidated that tensile stress applied to an HP Mg bar could hasten its in vitro corrosion, resulting in significant pitting and stress corrosion cracking [22]. This finding underscores the influence of tensile stress on the corrosion behavior of HP Mg. Aiming to alleviate stress and strain concentration at the junction of staple legs, Amano et al. innovated the crown design of FA sorb Mg™ staples, which has a more rounded shape that eliminates sharp bends, as illustrated in **Figure 1B** [18]. Subsequently, the study by Guo et al. revealed that the redesign of Zn-0.8Li-0.1Mn staples to incorporate chamfers, shown in **Figure 1C**, led to a primary concentration of residual stress on the legs and arc of the staple [5]. This structural optimization not only alters staple deformation but also impacts stress/strain distribution. Given the sensitivity of biodegradable materials to stress and strain, structural optimization presents a crucial method for reinforcing anastomosis with biodegradable staples.

Conclusion

Biodegradable surgical staples are designed to temporarily secure wounded tissue during the healing process, providing clear benefits over traditional permanent staples by minimizing post-surgical complications. The effectiveness of these staples, especially in gastrointestinal anastomosis, hinges on their ability to meet varied mechanical and biodegradation requirements, influenced by the healing rates and tissue types involved. Through careful selection of materials and structural refinement via finite element analysis, the practicality of biodegradable staples has been enhanced. Nonetheless, current researches on Mg/Zn-based alloys tend to overlook critical factors such as corrosion rate, age-hardening, creep, and corrosion fatigue. Addressing these aspects is crucial for a comprehensive evaluation of material suitability for gastrointestinal anastomosis applications, ensuring that biodegradable staples can reliably perform throughout the wound remodeling period.

References

[1] Wang M,Yang L, Zhu X. et al. Influence of enzymes on the in vitro degradation behavior of pure Zn in simulated gastric and intestinal fluidss. ACS Omega 2023;8:1331-1342.

[2] Milone M, Elmore U, Manigrasso M, et al. Circular versus linear stapling oesophagojejunostomy after laparoscopic total gastrectomy. A systematic review and meta-analysis. AM J Surg 2022;223:884-892.

[3] Chekan E, Whelan RL. Surgical stapling device–tissue interactions: what surgeons need to know to improve patient outcomes. Med Devices (Auckl) 2014;7:305-318.

[4] Zhang Y, Cao J, Lu M, et al. A biodegradable magnesium surgical staple for colonic anastomosis: In vitro and in vivo evaluation. Bioact Mater 2023;22:225-238.

[5] Guo H, Hu J, Shen Z, et al. In vitro and in

vivo studies of biodegradable Zn-Li-Mn alloy staples designed for gastrointestinal anastomosis. Acta Biomater 2021;121:713-723.

[6] Venezuela JJD, Johnston S, Dargusch MS. The Prospects for Biodegradable Zinc in Wound Closure Applications. Adv healthc mater 2019;8:e1900408.

[7] Wu H, Zhao C, Ni J, et al. Research of a novel biodegradable surgical staple made of high purity magnesium. Bioact Mater 2016;1:122-126.

[8] Ghosh S, More N, Kapusetti G. Surgical staples: Current state-of-the-art and future prospective. Med Nov Technol Devices 2022;16:100166.

[9] Yang N, Venezuela J, Almathami S, et al. Zinc-nutrient element based alloys for absorbable wound closure devices fabrication: Current status, challenges, and future prospects. Biomaterials 2022;280:121301.

[10] Qu S, Xia J, Yan J, et al. In vivo and in vitro assessment of the biocompatibility and degradation of high-purity Mg anastomotic staples. J Biomater Appl 2017;31:1203-1214.

[11] Xia J, Chen H, Yan, J, et al. High-Purity Magnesium Staples Suppress Inflammatory Response in Rectal Anastomoses. ACS Appl Mater Interfaces 2017;9:9506-9515.

[12] Zan R, Wang H, Ni J, et al. Multifunctional Magnesium Anastomosis Staples for Wound Closure and Inhibition of Tumor Recurrence and Metastasis. ACS Biomater Sci Eng 2021;7:5269-5278.

[13] Yan J, Chen Y, Yuan Q, et al. Comparison of the effects of Mg–6Zn and titanium on intestinal tract in vivo. J Mater Sci Mater Med 2013;24:1515-1525.

[14] Cheng Z, Li S, Zhang, Y, et al. Research of a biodegradable Mg-5Zn wire for anastomosis staples. Mater Lett 2023;352:135173.

[15] Song L, Gao M, Tan L, et al. Application Potential of Mg–Zn–Nd Alloy as a Gastrointestinal Anastomosis Nail Material. Acta Metall Sin 2022;35:609-620.

[16] Gao M, Na D, Ni X, et al. The mechanical property and corrosion resistance of Mg-Zn-Nd alloy fine wires in vitro and in vivo. Bioact Mater 2021;6:55-63.

[17] Zhang H, Shen Y, Ding Y, et al. In vitro corrosion and in vivo behavior of high strength Mg-6Zn-1Mn alloy wire for gastrointestinal anastomosis nail application. Biomater Adv 2022;142:213159.

[18] Amano H, Hanada K, Hinoki A, et al. Biodegradable Surgical Staple Composed of Magnesium Alloy. Sci Rep 2019;9:14671.

[19] Amano H, Miyake K, Hinoki A, et al. Novel zinc alloys for biodegradable surgical staples. World J Clin Cases 2020;8:504-516.

[20] Henning W, Kerstin R, Andreas W, et al. Correction to: Biodegradable magnesium-based screw clinically equivalent to titanium screw in hallux valgus surgery: short term results of the first prospective, randomized, controlled clinical pilot study. Biomed Eng OnLine 2020;19:86.

[21] Haude M, Toelg R, Lemos PA, et al. Sustained safety and performance of a second-generation sirolimus-eluting absorbable metal scaffold: Long-term data of the BIOSOLVE-II first-in-man trial at 5 years. Cardiovasc Revasc Med 2021;38:106-110.

[22] Gao Y, Wang L, Li L, et al. Effect of stress on corrosion of high-purity magnesium in vitro and in vivo. Acta Biomater 2019;83:477-486.